frontiers in Earth Science

ORIGINAL RESEARCH
published: 08 October 2015
doi: 10.3389/feart.2015.00060

Physiology, Fe(II) oxidation, and Fe mineral formation by a marine planktonic cyanobacterium grown under ferruginous conditions

Elizabeth D. Swanner[1, 2], Wenfang Wu[1, 3], Likai Hao[1], Marina Lisa Wüstner[1], Martin Obst[1], Dawn M. Moran[4], Matthew R. McIlvin[4], Mak A. Saito[4] and Andreas Kappler[1]*

[1] Department of Geosciences, University of Tübingen, Tübingen, Germany, [2] Department of Geological and Atmospheric Sciences, Iowa State University, Ames, IA, USA, [3] Key Laboratory of the Earth's Deep Interior, Institute of Geology and Geophysics, Chinese Academy of Sciences, Beijing, China, [4] Marine Chemistry and Geochemistry Department, Woods Hole Oceanographic Institution, Woods Hole, MA, USA

OPEN ACCESS

Edited by:
Dina M. Bower, NASA's Goddard Space Flight Center and University of Maryland, USA

Reviewed by:
John Senko, The University of Akron, USA
Trinity L. Hamilton, University of Cincinnati, USA

***Correspondence:**
Elizabeth D. Swanner, Department of Geological and Atmospheric Sciences, Iowa State University, 253 Science I, Ames, IA 50011, USA
eswanner@iastate.edu

Specialty section:
This article was submitted to Biogeoscience, a section of the journal Frontiers in Earth Science

Received: *30 July 2015*
Accepted: *17 September 2015*
Published: *08 October 2015*

Citation:
Swanner ED, Wu W, Hao L, Wüstner ML, Obst M, Moran DM, McIlvin MR, Saito MA and Kappler A (2015) Physiology, Fe(II) oxidation, and Fe mineral formation by a marine planktonic cyanobacterium grown under ferruginous conditions. Front. Earth Sci. 3:60. doi: 10.3389/feart.2015.00060

Evidence for Fe(II) oxidation and deposition of Fe(III)-bearing minerals from anoxic or redox-stratified Precambrian oceans has received support from decades of sedimentological and geochemical investigation of Banded Iron Formations (BIF). While the exact mechanisms of Fe(II) oxidation remains equivocal, reaction with O_2 in the marine water column, produced by cyanobacteria or early oxygenic phototrophs, was likely. In order to understand the role of cyanobacteria in the deposition of Fe(III) minerals to BIF, we must first know how planktonic marine cyanobacteria respond to ferruginous (anoxic and Fe(II)-rich) waters in terms of growth, Fe uptake and homeostasis, and Fe mineral formation. We therefore grew the common marine cyanobacterium *Synechococcus* PCC 7002 in closed bottles that began anoxic, and contained Fe(II) concentrations that span the range of possible concentrations in Precambrian seawater. These results, along with cell suspension experiments, indicate that Fe(II) is likely oxidized by this strain via chemical oxidation with oxygen produced during photosynthesis, and not via any direct enzymatic or photosynthetic pathway. Imaging of the cell-mineral aggregates with scanning electron microscopy (SEM) and confocal laser scanning microscopy (CLSM) are consistent with extracellular precipitation of Fe(III) (oxyhydr)oxide minerals, but that >10% of Fe(III) sorbs to cell surfaces rather than precipitating. Proteomic experiments support the role of reactive oxygen species (ROS) in Fe(II) toxicity to *Synechococcus* PCC 7002. The proteome expressed under low Fe conditions included multiple siderophore biosynthesis and siderophore and Fe transporter proteins, but most siderophores are not expressed during growth with Fe(II). These results provide a mechanistic and quantitative framework for evaluating the geochemical consequences of perhaps life's greatest metabolic innovation, i.e., the evolution and activity of oxygenic photosynthesis, in ferruginous Precambrian oceans.

Keywords: Fe(II) oxidation, cyanobacteria, proteomics, reactive oxygen species (ROS), siderophores, Banded Iron Formation (BIF), Great Oxidation Event (GOE)

Introduction

Iron (Fe) is an essential element to all life, but its bioavailability in aqueous environments has shifted throughout Earth's history, primarily in response to the oxidation of surface waters. Average Fe concentrations of 540 pmol kg^{-1} limit the productivity of primary producers dwelling in the photic zone of many regions of the modern ocean (e.g., Boyd et al., 2000). During the Precambrian Eon [4.6 billion years (Gy) ago to 541 million years (My) ago], however, anoxic and ferruginous oceans were a persistent feature of Earth's surface (Canfield, 1998; Planavsky et al., 2011; Poulton and Canfield, 2011), where Fe(II) concentrations in the deep oceans are estimated to have been between 40 and 120 μM (Canfield, 2005). As cyanobacteria are the only clade of oxygen-evolving photosynthetic organisms in the microbial domains of bacteria and archaea, it is generally accepted that they are the modern remnants of the evolutionary most ancient organisms capable of oxygenic photosynthesis (Blankenship, 1992). Yet because of pervasive surface oxidation, fewer modern environments exist today in which ferruginous waters [i.e., containing free Fe(II)] enter sunlit, circumneutral pH environments. Therefore, most studies of the interaction of Fe with cyanobacteria have focused on oxic conditions, where Fe(III) is a limiting nutrient due to its poor solubility. We therefore have little physiological context for understanding the activity of cyanobacteria under ferruginous conditions, yet this is crucial for evaluating their activity in Precambrian oceans.

Globally, marine planktonic cyanobacteria, such as the predominant *Prochlorococcus* and *Synechococcus* species account for a major portion of modern marine primary productivity (Partensky et al., 1999), and if planktonic cyanobacteria existed on the early Earth, they should have made significant contributions to oxygen production (Olson et al., 2013). Because abiotic O_2 production was not significant under early Earth conditions (Haqq-Misra et al., 2011; Pecoits et al., 2015), it is thought that geochemical evidence for atmospheric and surface water oxidation in the Precambrian is evidence for the activity of cyanobacteria, or organisms capable of oxygenic photosynthesis at that time (Buick, 1992). At the time of the Great Oxidation Event (GOE) at around 2.4 Ga, atmospheric oxygen concentrations underwent a permanent rise, exceeding 10^{-5} present atmospheric levels (PAL; Pavlov and Kasting, 2002; Bekker et al., 2004). However, recent work has documented evidence that periodic, localized atmospheric oxygen levels exceeded 10^{-5} PAL, and that oxygen was present in marine surface waters up to 600 million years before the GOE (Anbar et al., 2007; Wille et al., 2007; Kendall et al., 2010; Crowe et al., 2013; Reinhard et al., 2013; Planavsky et al., 2014).

The inferred presence and activity of cyanobacteria in the Archean Eon (4 to 2.5 Gy ago) requires that marine cyanobacteria would have been exposed to periodic upwelling or diffusion of Fe(II)-rich waters into the photic zone (Holland, 1973; Beukes and Gutzmer, 2008). Sedimentological evidence suggests that Fe(II), sourced to the deep Precambrian oceans from hydrothermal leaching of oceanic crust (Bau and Moeller, 1993), upwelled toward the surface ocean and was oxidized and deposited as poorly soluble Fe(III) (oxyhydr)oxide minerals (Beukes and Klein, 1992). Because abiotic mechanisms for Fe(II) oxidation seem to have limited relevance under early Earth conditions (Konhauser et al., 2007), much emphasis has been placed on biological mechanisms (for a recent review, see Posth et al., 2013). Specifically, the oxidation of Fe(II) under anoxic conditions by anoxygenic phototrophic organisms (photoferrotrophs) (Widdel et al., 1993) has received considerable attention. But evidence for oxygen several 100 years before the GOE bring back to the foreground the original idea that photosynthetic oxygen, produced by oxygenic phototrophs such as early cyanobacteria, was the oxidant for Fe(II) (i.e., Cloud, 1968).

Some investigations have addressed the mechanism of Fe(II) oxidation and Fe mineral formation by mat-forming cyanobacterial communities in modern Fe(II)-rich springs or other settings, or in cyanobacteria isolated from these sites (Pierson et al., 1999; Trouwborst et al., 2007; Brown et al., 2010; Parenteau and Cady, 2010; Ionescu et al., 2014). However, the suggestion that Fe(II) oxidation could occur in cyanobacteria capable of using the evolutionarily more ancient anoxygenic photosynthetic pathway (Olson and Pierson, 1987a,b) lacks support from experiments with modern cyanobacteria (Cohen et al., 1986; Trouwborst et al., 2007). Furthermore, recent work has documented that the relationship between cyanobacteria, Fe(II), and photosynthetic oxygen production is influenced by the production of toxic reactive oxygen species (ROS) when oxygen reacts with Fe(II) (Swanner et al., 2015). Therefore, in order to ascertain to what extent cyanobacteria may have been involved in both Precambrian oxygen production and BIF deposition, the multi-layered relationship between cyanobacteria, Fe(II), toxicity, oxygen production, Fe(II) oxidation, and Fe (bio)mineralization need to be considered.

As oxygenic phototrophs, cyanobacteria have a large Fe quota: 22 atoms of Fe per complex are needed to sustain electron flow through PSI and PSII (Raven, 1990). Therefore, modern cyanobacteria show diverse intracellular Fe quotas (Twining et al., 2004; Twining and Baines, 2013). Cyanobacteria also possess numerous physiological adaptations to Fe limitation under oxic conditions, such as substitution of Fe-free flavodoxin electron-transfer protein for Fe-containing ferrodoxin, (Erdner et al., 1999). Expression of siderophores, small molecules that bind Fe with high affinity, has been observed in some cyanobacteria under Fe limitation (Wilhelm and Trick, 1994; Wilhelm, 1995; Wilhelm et al., 1996, 1998), and siderophores may help cyanobacteria adapt to Fe limited surface waters (Sorichetti et al., 2014). Siderophores or other biologically-secreted Fe-binding ligands that can maintain Fe(III) as a soluble species likely complex much of the Fe in oxic surface waters (Gledhill and Van Den Berg, 1994; Van Den Berg, 1995; Wu and Luther Iii, 1995), and can drive photochemical redox-cycling of Fe(III) to Fe(II) (Barbeau et al., 2001, 2003; Barbeau, 2006), as well as biological reduction of Fe(III) to Fe(II) prior to Fe(II) uptake by the cell (Kranzler et al., 2011; Lis et al., 2015). While siderophore production is documented for numerous cyanobacteria under Fe limitation, it is unknown whether similar Fe-binding molecules are secreted under ferruginous conditions,

but Fe-binding ligands could also play a role in controlling the solubility, reactivity, and transport of hydrothermally-derived Fe (Toner et al., 2009; Sander and Koschinsky, 2011; Conway and John, 2014; Horner et al., 2015), relevant for understanding the dynamics of the Precambrian Fe cycle.

This study evaluates the growth, oxygen production, Fe(II) oxidation, Fe mineral formation, various physiological characteristics, and protein expression of planktonic marine cyanobacterium, *Synechococcus* PCC 7002, when grown under ferruginous conditions. These experiments are used to inform the physiological response of cyanobacteria to anoxic, Fe(II)-rich conditions, their role in Fe(II) oxidation, and their contribution to Fe (bio)mineralization. We use these results to infer how cyanobacterially-mediated Fe(II) oxidation in Precambrian oceans might have occurred, and what potential geochemical/mineralogical consequences their activity had that may be recorded in the rock record. *Synechococcus* PCC 7002 was used in this study as a model organism for understanding the physiological behavior of cyanobacteria in an ancient, ferruginous ocean. As as a coastal representative of *Synechococcus*, it does not cluster near the base the phylogenetic tree of cyanobacteria (Schirrmeister et al., 2015). However, this microbe may be as relevant a model organism as any extant cyanobacterium, since ancient oceans were likely not the extremely oligotrophic low nutrient environments observed today, and phylogenetic analyses also imply that abundant open ocean cyanobacteria are also not the most basal clades (Blank and Sánchez-Baracaldo, 2010).

Methods

Medium and Growth Assessment

Synechococcus PCC 7002 is a halotolerant strain isolated from mud on Magueyes Island, Puerto Rico (Van Baalen, 1962). An axenic culture of *Synechococcus* PCC 7002 was cultivated under static conditions on Marine Phototroph (MP) medium in acid-washed and sterilized glass serum bottles (1N HCl; 24 h) at 24°C under an irradiance of 12.8 μmol photons m^{-1} s^{-1} from a standard 40W tungsten light bulb (Wu et al., 2014). Additions were made after autoclaving and degassing (N_2/CO_2, 90:10 v/v), and included 3 mg L^{-1} filtered ferric chloride, selenium and tungstate solution (Widdel, 1980), 0.5 mM $Na_2S_2O_3$, and 1 mL each of vitamin and trace element solutions (described in Wu et al., 2014). This medium did not contain EDTA or other metal chelates. Fe(II) amendments were added from a sterile $FeCl_2$ stock, and the medium was filtered through a 0.2 μm polystyrene filter (Millipore Stericup) in a glovebox after precipitation of Fe(II) with phosphate and carbonate present in the medium (Wu et al., 2014). Final Fe(II) concentrations varied based on the saturation indices of these phases, and the amount of $FeCl_2$ added. The Fe(II) content of each batch of medium was therefore determined empirically with the ferrozine method (see below) prior to the start of each experiment. In medium containing $FeCl_2$, the trace elements, vitamins, and supplements were added after filtration to avoid their removal via sorption to precipitated phases. For growth experiments, 80 mL of medium was filled into 100 mL glass Schott bottles in a glovebox (100% N_2), sealed with a butyl rubber stopper, and the headspace was flushed with N_2/CO_2 (90:10). For proteomics experiments, cells were first cultivated in the medium described above without Fe(II), but with ferric ammonium citrate substituted for ferric chloride at a concentration of 6 mg L^{-1}. Cells were then inoculated into glass serum bottles with no added Fe(III), but which contained either 170 μM $FeCl_2$ added as described above (high Fe), or simply Fe(II) added from the trace element solution (low Fe; final concentration 7.5 μM). In all experiments, cyanobacteria cultures were degassed for 5 min. in the dark (N_2/CO_2, 90:10 v/v) prior to inoculation into anoxic, Fe(II)-containing medium.

Growth was monitored by optical density (OD) measurements at 750 nm with a photospectrometer (Spekol 1300, Analytik Jena) for cultures containing ≤100 μM Fe(II). Cell numbers of experiments with >100 μM Fe(II) were determined from direct counts of images of autofluorescent *Synechococcus* PCC 7002 cells after Fe(III) minerals were dissolved with an oxalate solution (Wu et al., 2014). Images were acquired on a Leica DM5500B fluorescence microscope using the Y3 filter. Additionally, cells mL^{-1} values were calculated from OD measurements via a standard curve relating OD measurements to direct counts of cells grown in medium without additional $FeCl_2$. Pigments were extracted from log-phase cultures with 4°C 90% methanol and measured in a WTW photoLab 6600 UV-Vis series spectrophotometer just prior to complete oxidation of the initial Fe(II) added to the growth medium. The chlorophyll *a* and carotenoid contents were determined according to equations in Sakamoto and Bryant (1998). Chlorophyll *a* contents were related to OD via a standard curve derived from measurement of both parameters on cultures of varying cell density for cultures that contained less than 100 μM Fe(II) initially. For cultures with ≥100 μM Fe(II) initially, direct cell counts were again performed after oxalate digestion.

Aqueous Geochemical Measurements in Growth Experiments

Samples from growth experiments containing ≥1 mM total Fe were stabilized in anoxic 1N HCl and stored in a glovebox until analysis for Fe(II) with 0.1% ferrozine in 50% ammonium acetate. Samples containing <1 mM total Fe were reacted directly with ferrozine in a glovebox after sampling. Absorption measurements were made at 562 nm after samples were centrifuged (16,000 × g) to pellet cells and the solid Fe phase (i.e., Fe(III) minerals), as the absorption of light by *Synechococcus* PCC 7002 cells interfered with the absorption of the Fe(II)-ferrozine complex at 562 nm. Oxygen concentrations in growth experiments were measured using a Fibox fiber optic oxygen transmitter and non-invasive optical oxygen sensors glued into the media bottles, and utilized a 2-point calibration provided by the manufacturer (PreSens Precision Sensing, Regensburg, Germany).

Cell Suspension Experiments

To measure intracellular Fe, *Synechococcus* PCC 7002 was grown in a large volume (ca. 250 mL) of MP medium with ferric ammonium citrate as an Fe(III) source to late exponential phase. Cells were harvested by centrifugation (7197 × g; 10 min) and washed three times in a non-growth buffer at pH 7

(i.e., MP medium without trace elements, Fe(III), vitamins or supplements, NH_4Cl or K_2HPO_4, or bicarbonate), and resuspended in fresh buffer to a concentration of 1×10^8 cells ml^{-1}. Oxygen was removed from light-shielded washed cells by bubbling the suspensions for 5 min with N_2/CO_2 (90: 10). Fe(II) was added to the suspensions from an anoxic stock of $FeCl_2$ prior to light exposure. Incubations to measure intracellular Fe concentrations were similar to those designed to detect intracellular reactive oxygen species (ROS) as described in Swanner et al. (2015). Here, samples of cells were taken before and after a 1-h light incubation (25 μmol photons m^{-2} s^{-1}) from suspensions with different initial concentrations of $FeCl_2$ (none, 10, 100, and 1000 μM). Samples were immediately spun in 0.2 μm nylon centrifuge tube filters (Costar Spin-X, Corning International) at 16,000 × g for 3 min to separate cells from the Fe in solution. Cells suspended on the filter were then washed on the filter with a Ti-EDTA-citrate solution to remove sorbed Fe (Tang and Morel, 2006), and rinsed once with MP buffer. Cells were dried overnight at 60°C, then weighed into Teflon beakers and digested with concentrated trace metal grade (TMG) HNO_3 and 30% H_2O_2. Residues were resuspended in 8N TMG HNO_3, and further diluted in 2% TMG HNO_3 for analysis. Iron measurements were carried out by ICP-MS (ThermoFisher XSeries2; detection limit of 0.807 ppm Fe).

Cell suspension experiments to test for anoxygenic photosynthesis by *Synechococcus* PCC 7002 were prepared as described above. Incubations of cell suspensions were carried out in a Qubit Systems OX1LP Dissolved O_2 Package (Kingston, ON, Canada). Oxygen was quantified with a 2-point calibration performed according to the manufacturer's instructions. Fe(II) was added to the suspensions from an anoxic $FeCl_2$ stock to a final concentration of 100 μM prior to light exposure. Fe(II) concentrations were determined on samples removed from the cell stand with a syringe during hour-long incubations at 20–25°C under an irradiance of 20.9 μmol photons m^{-1} s^{-1} light. To stabilize Fe(II) for measurement, 200 μL of the sample was immediately mixed with 200 μL of 2 M HCl. Cells were removed by centrifugation at 16,000 × g for 10 min using 0.22 μm nylon centrifuge tube filter (Cosar spin-X, Corning, International). Fe(II) was quantified using the ferrozine assay (Stookey, 1970; Dippon et al., 2012). To test for anoxygenic photosynthesis, DCMU (3-(3,4-dichlorophenyl)-1,1-dimethylurea) prepared in ethanol was added to a final concentration of 8 μM in suspensions. DCMU blocks electron transfer from Photosystem II to plastiquinone, and allows to determine whether Fe(II) is oxidized via a potential anoxygenic pathway of Photosystem I. No experiments were performed in the dark.

Proteomics Analysis

Triplicate inoculations of *Synechococcus* PCC 7002 on MP medium with low or high Fe treatments were made and allowed to grow until all Fe(II) had just been oxidized (3 days), in the case of high Fe treatments. The biomass was then harvested by centrifugation (7197 × g; 10 min) and washed with MP buffer. The biomass was then loaded into filter tubes and treated with Ti-EDTA-citrate as described above for the intracellular Fe determination experiment. Washed cells were then stored at −20°C until extraction for proteomics analysis.

Samples were resuspended with 500 μl of 1% SDS extraction buffer (1% SDS, 0.1M Tris/HCL pH 7.5, 10 mM EDTA). Each sample was incubated at room temperature for 15 min, heated at 95°C for 10 min, and shaken at room temperature, 350 rpm for 1 h. The protein extract was decanted and filter tube rinsed with an additional 500 μl of extraction buffer. Each sample and corresponding rinse were combined in a new tube and centrifuged (14100 × g; 20 min) at room temperature. The supernatants were removed and concentrated by membrane centrifugation to approximately 300 μL in 6 mL, 5 K MWCO Vivaspin units (Sartorius Stedim, Goettingen, Germany). Each sample was precipitated with cold 50% methanol, 50% acetone, and 0.5 mM HCL for 3 days at −20°C, then centrifuged at 14100 × g for 30 m at 4°C, decanted and dried by vacuum concentration (Thermo Savant Speedvac) for 10 min or until dry. Pellets were resuspended in 1% SDS extraction buffer and left at room temperature for 1 h to completely dissolve. Total protein was quantified (Bio-Rad DC protein assay, Hercules, CA) with BSA as a standard.

Extracted proteins were purified from SDS detergent, reduced, alkylated, and trypsin digested while embedded within a polyacrylamide tube gel, modified from a previously published method (Lu and Zhu, 2005). A gel premix was made by combining 1 M Tris HCL (pH 7.5) and 40% Bis-acrylimide L 29:1 (Acros Organics) at a ratio of 1:3. The premix (103 μl) was combined with an extracted protein sample (35–200 μg), TE, 7 μl 1% APS and 3 μl of TEMED (Acros Organics) to a final volume of 200 μl. After 1 h of polymerization at RT, 200 μl of gel fix solution (50% ethanol, 10% acetic acid in liquid chromatography-mass spectrometry (LC-MS) grade water) was added to the top of the gel and incubated at RT for 20 min. Liquid was then removed and the tube gel was transferred into a new 1.5 mL microtube containing 1.2 mL of gel fix solution and then incubated at room temperature, then spun at 350 rpm in a Thermomixer R (Eppendorf) for 1 h. The gel fix solution was then removed and replaced with 1.2 mL destain solution (50% methanol, 10% acetic acid in H_2O) and incubated at 350 rpm for 2 h at room temperature. The liquid was then removed, and gel cut into 1 mm cubes, which were added back to tubes containing 1 mL of 50:50 acetonitrile:25 mM ammonium bicarbonate incubated for 1 h at 350 rpm at room temperature. The liquid was removed and replaced with fresh 50:50 acetonitrile:ammonium bicarbonate and incubated at 16°C and 350 rpm overnight. The above step was repeated for 1 h the following morning. Gel pieces were then dehydrated twice in 800 μl of acetonitrile for 10 min at room temperature, and dried for 10 min in a ThermoSavant DNA110 Speedvac after removing the solvent. Then, 600 μl of 10 mM DTT in 25 mM ammonium bicarbonate was added to reduce proteins incubating at 56°C, 350 rpm for 1 h. Unabsorbed DTT solution was then removed, and the volume measured. Gel pieces were washed with 25 mM ammonium bicarbonate, and 600 μl of 55 mM iodacetamide was added to alkylate proteins at room temperature and 350 rpm for 1 h. Gel cubes were then washed with 1 mL ammonium bicarbonate for 20 min at 350 rpm and room

temperature. Acetonitrile dehydrations and Speedvac drying were repeated as above. Trypsin (Promega #V5280) was added in an appropriate volume of 25 mM ammonium bicarbonate to rehydrate and submerse gel pieces at a concentration of 1:20 μg trypsin:protein. Proteins were digested overnight at 350 rpm and 37°C. Unabsorbed solution was removed and transferred to a new tube. Then, 50 μl of peptide extraction buffer (50% acetonitrile, 5% formic acid in water) was added to gels, incubated for 20 min at room temperature, and then centrifuged at 14,100 × g for 2 min. The supernatant was collected and combined with unabsorbed solution. The above peptide extraction step was repeated, combining all supernatants. Combined protein extracts were centrifuged at 14,100 × g for 20 min, and the supernatants were transferred into a new tube and dehydrated down to approximately 10–20 μl in the Speedvac. Concentrated peptides were then diluted in 2% acetonitrile 0.1% formic acid in water for storage until analysis. All water used in the tube gel digestion protocol was LC-MS grade, and all plastic microtubes were ethanol rinsed and dried prior to use.

Protein extracts from the biological triplicates were analyzed by LC-MS (Michrom Advance HPLC coupled to a Thermo Scientific Fusion Orbitrap mass spectrometer with a Thermo Flex source). Each sample was concentrated onto a trap column (0.2×10 mm ID, 5 μm particle size, 120 Å pore size, C18 Reprosil-Gold, Dr. Maisch GmbH) and rinsed with 100 μL 0.1% formic acid, 2% acetonitrile, and 97.9% water before gradient elution through a reverse phase C18 column (0.1 × 500 mm ID, 3 μm particle size, 120 Å pore size, C18 Reprosil-Gold, Dr. Maisch GmbH) at a flow rate of 250 nL/min. The chromatography consisted of a nonlinear 190 min gradient from 5 to 95% of a buffer containing 0.1% formic acid in acetonitrile. The remaining buffer was made up of 0.1% formic acid in water (all solvents were Fisher Optima grade). The mass spectrometer was set to perform MS scans on the orbitrap (240000 resolution at 400 m/z) with a scan range of 380 m/z to 1580 m/z. MS/MS was performed on the ion trap using data-dependent settings (top speed, dynamic exclusion 15 s, excluding unassigned and singly charged ions, precursor mass tolerance of ± 3 ppm, with a maximum injection time of 50 ms). Search results were performed using Proteome Discoverer 1.4 (Thermo Scientific) and Scaffold 4.0 (Proteome Software Inc.).

Microscopic and Mineralogical Analyses

Two samples for scanning electron microscopy (SEM) were taken from a growth culture with a starting concentration of ca. 5 mM Fe(II) near the beginning and at the end of the Fe(II) oxidation phase, and were fixed in glutaraldehyde. After fixation, samples were washed with filtered water. Fixed cells were immobilized on poly-l-lysine coated glass cover slips and then dehydrated in an ethanol series (30, 50, 90%, 3 × 100%) and critical point dried. Prior to microscopy, the glass cover slips were attached to aluminum stubs with carbon tape and sputter-coated with 6 nm platinum. Secondary electron images were collected on a Leo 1450VP SEM (Carl Zeiss SMT AG, Germany) operated at an accelerating voltage of 5 kV and a probe current of 9 pA.

Samples of *Synechococcus* PCC 7002 grown with Fe(II) were imaged by confocal laser scanning microscopy (CLSM; Leica SPE, Mannheim, Germany) just after the initial ca. 0.5 mM Fe(II) had been oxidized. A 635 nm laser was used to excite autofluorescence of *Synechococcus* PCC 7002, with an emission peak at 660 nm (detected range of emission 640–700 nm). The Fe(III) minerals were imaged using the reflection signal of the 488 nm laser. Soluble/ligand-bound Fe(III) was stained with of turn-on type, highly sensitive and selective fluorescence probe, (Mao et al., 2007, 2010), added to a final concentration of 1 μM, which was excited with the 488 nm laser (emission range from 500 to 560 nm). The Auto-Quant™ deconvolution algorithm implemented in the LEICA LAS AF software was applied to blind deconvolution the 3D image stacks (Schmid et al., 2014).

Images from fluorescent cell counts were analyzed for average cell size using the 3D Objects Counter from IMAGEJ (Abràmoff et al., 2004). ScatterJ, a plugin for correlation and co-localization analysis of species-specific maps that was developed for IMAGEJ (Zeitvogel et al., 2014), was used to analyze the spatial relationships of species detected using fluorescence dyes with CLSM. An angle-deviation map from a slope of 1 was calculated from the 3D datasets of the autofluorescence signal and the fluorescence signal of the Fe(III) fluorescence probe using ScatterJ. Signal intensities <0.2% (grayscale value of 5 in an 8 bit image) were considered as noise and excluded from the plots. Thereby, positive angle-deviations indicate higher Fe(III)-signals per autofluorescence signal, whereas negative angles indicate a lower Fe(III)-signal.

Results

Growth and Physiological Indicators of *Synechococcus* PCC 7002 under Ferruginous Conditions

Growth of *Synechococcus* PCC 7002 in closed-bottle incubations was observed at up to 7000 μM initial Fe(II), but we were not able to cultivate this strain at higher Fe(II) concentrations (i.e., at 8000 μM), based on the absence of growth indicators (i.e., visible cell density) and no significant Fe(II) oxidation (which would indicate photosynthetic oxygen production). In these experiments, cultures with the lowest concentrations of Fe(II) turned green in the first few days, but at higher concentrations of Fe(II), the culture was dominated by rust-colored Fe(III) minerals (**Figure 1**). This finding implies a higher density of cells when Fe(II) concentrations are initially lower, copacetic with the lower cell numbers in the first days after inoculation when initial Fe(II) concentrations were higher (**Figure 2**). Once Fe(II) was oxidized, cell densities in incubations with 4800 μM initial Fe(II) reached similar values to experiments with only 7.5 μM Fe(II) (**Figure 2**). Fluorescent microscopic imaging documented that cell sizes were significantly smaller for cultures grown with higher initial Fe(II) concentrations (**Table 1**). Both the chlorophyll *a* and carotenoid content of cells also considerably decreased when grown with initial Fe(II) concentrations of 70 μM or higher (**Table 1**).

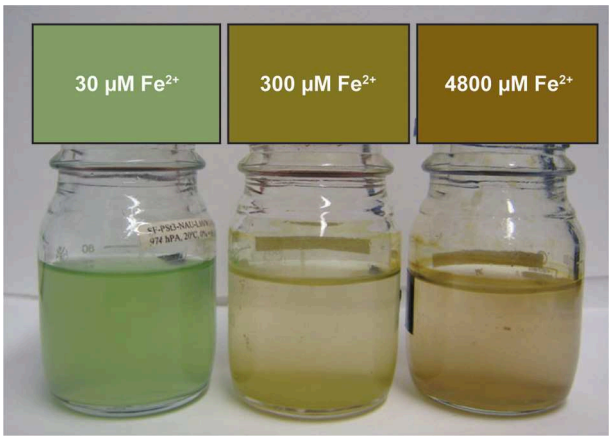

FIGURE 1 | Images of *Synechococcus* PCC 7002 growing in sealed bottles that began anoxic with different concentrations of Fe(II). These images were taken 5 days after inoculation.

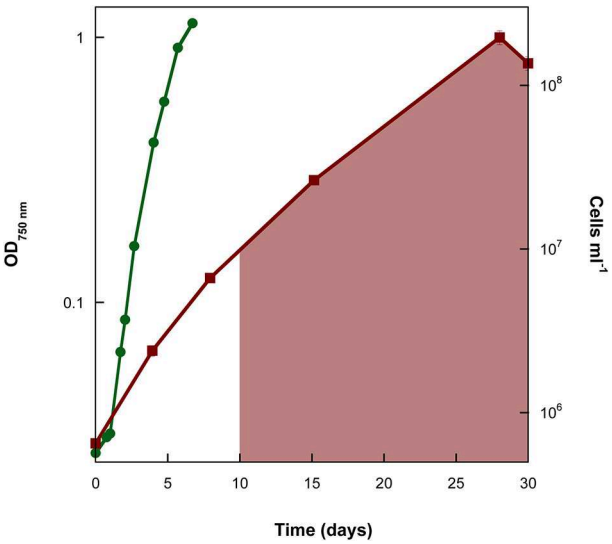

FIGURE 2 | Cell counts of a representative replicate of the experiment where the marine cyanobacterium *Synechococcus* PCC 7002 was cultivated under conditions that began anoxic with 4800 μM Fe(II). Cell numbers reach similar values to the experiment with 7.5 μM Fe(II) once all of the Fe(II) has been oxidized (shaded area denotes time when Fe(II) was no longer detectable by ferrozine).

Previously, a 2-fold increase in intracellular ROS contents was detected when cells of photosynthesizing *Synechococcus* PCC 7002 were incubated with 100 μM Fe(II), as compared to a control with no added Fe(II), as well as a 4-fold increase when extracellular Fe(II) concentrations reached 1000 μM Fe(II) (Swanner et al., 2015). To determine if Fe(II) uptake was linked to ROS production in Fe(II) incubations, we incubated photosynthesizing *Synechococcus* PCC 7002 with different concentrations of Fe(II) for 1 h, in a similar experiment to that in which elevated ROS concentrations were measured by Swanner et al. (2015). After the incubation,

TABLE 1 | Difference in cell size and pigment concentrations when *Synechococcus* PCC 7002 was grown with different Fe(II) concentrations.

Fe(II) (μM)	Mean	*SE*	*n*	*P*-value	Significance
AVERAGE CELL SIZE (μm²)					
300	3.62	0.18	42		
4800	2.84	0.12	41	0.00068	***
CHLOROPHYLL A CONCENTRATION (μg/CELL)					
7.5	4.58E-08	3.80E-09	3		
30	5.21E-08	1.65E-08	3	0.7234	
70	8.50E-09	4.39E-08	3	0.0011	**
7000	6.91E-09	2.04E-08	3	0.0001	***
CAROTENOID CONCENTRATION (μg/CELL)					
7.5	3.50E-09	4.00E-10	3		
30	3.29E-09	1.13E-09	3	0.868	
70	5.13E-10	2.90E-09	3	0.0005	***
7000	5.24E-10	1.60E-09	3	0.0001	***

*Asterisks indicate whether the mean of measurements at one Fe(II) concentration is significantly different the second. The comparison was made using an unpaired t-test: **very significant $p < 0.01$; ***extremely significant $p < 0.001$.*

TABLE 2 | Intracellular and sorbed Fe concentrations when suspensions of *Synechococcus* PCC 7002 were incubated in light with different initial Fe(II) concentrations.

Initial Fe(II) (μM)	Intracellular Fe (fmol/cell)	Sorbed Fe (fmol/cell)
0	0.142 (37%)	0.055 (38%)
10	0.090 (16%)	0.064 (49%)
100	0.036 (2%)	0.068 (35%)
1000	0.025 (<0.01%)	0.103 (12%)

Values in parentheses are the percentages of total Fe measured in the system that is present in each phase.

we measured the intracellular and sorbed Fe contents by ICP-MS. We observed lower intracellular Fe contents when extracellular Fe(II) concentrations were higher (**Table 2**), the same conditions under which enhanced intracellular ROS were previously observed (Swanner et al., 2015). The amount of Fe sorbed per cell increased slightly at higher initial Fe(II) concentrations despite lower intracellular Fe contents (**Table 2**).

Proteomics of *Synechococcus* PCC 7002 under High Fe and Low Fe Treatments

In order to further investigate the mechanism of Fe(II) toxicity, and to understand the effect of Fe concentration and speciation on siderophore production by this strain, *Synechococcus* PCC 7002 was grown with varying initial concentrations of Fe(II), either 7.5 μM (low Fe) or 170 μM (high Fe), and the expressed proteins under each growth condition were detected and quantified. Overall, 1631 proteins were detected out of the 2824 coded for in the genome, implying that 56% of the genome was expressed under these two conditions (see Supplementary Table 1 for Global Proteome spectral count data). The analysis utilized a stringent criteria for protein identification of 99% minimum peptide and protein probabilities, less than 1% false discovery

ferredoxin-like protein gi|170076880
protochlorophyllide reductase iron-sulfur ATP-binding protein gi|170078942
iron compound TonB-dependent receptor gi|170077260
ferredoxin gi|170079270
pyruvate:ferredoxin flavodoxin oxidoreductase gi|170078052
ferredoxin-thioredoxin reductase variable chain gi|170079106
ferredoxin 2Fe-2S gi|170078790
ferredoxin gi|170077629
FeS cluster assembly accessory/regulatory protein gi|170076856
ferredoxin [2Fe-2S] II gi|170077248
ferric uptake regulator gi|170078257
putative ferredoxin 2Fe-2S gi|170077629
photosystem II 12 kDa extrinsic protein PsbU gi|170076950
ferredoxin-thioredoxin reductase catalytic chain gi|170078457
ferredoxin gi|170079268
Mn-superoxide dismutase gi|170076871
photosystem I protein PsaE gi|159162852
photosystem I reaction center subunit III, PsaF gi|170077629
phycocyanobilin:ferredoxin oxidoreductase gi|170078825
photosystem II manganese stabilizing protein PsbO gi|170076897
thioredoxin family protein gi|170076921
light-repressed protein LrtA gi|170076891
ferredoxin-NADP reductase gi|170077475
ABC transporter ATP-binding protein gi|170077249
catalase/peroxidase HPI gi|170079017
recombinase A gi|170077054
Dps family DNA-binding stress response protein gi|170076667
photosystem II reaction center protein Psb28 gi|170077874
bacterioferritin comigratory protein gi|170077726
ferrochelatase gi|170079183
bacterioferritin gi|170079257
iron transport protein gi|170079102
bacterioferritin gi|170079258
ABC transporter family protein gi|170079375
ABC transporter ATPase gi|170077798
ABC transporter family protein gi|170078787
DNA repair protein RecN gi|170077077
Na/H+ antiporter gi|170077202
recombination protein F gi|170078873
outer membrane TonB-dependent hemoglobin/transferrin/lactoferrin receptor family protein gi|170076551
flavodoxin FldA gi|170077906
TonB dependent receptor gi|170076476
ferrichrome-iron receptor; TonB-dependent siderophore receptor gi|170076573
TonB-dependent siderophore receptor gi|170076608
TonB-dependent siderophore receptor gi|170076568
siderophore biosynthesis protein gi|170076493
siderophore biosynthesis protein; N-monooxygenase gi|170076491
lucA/lucC family siderophore biosynthesis protein gi|170076489
iron compound ABC transporter, ATP-binding protein gi|170076550
ABC transporter gi|170077493
TonB family protein gi|170076560
ABC transporter, periplasmic iron-binding lipoprotein gi|170076553
Iron stress-induced chlorophyll-binding protein gi|400071
ABC transporter ATP-binding protein gi|170078821
periplasmic binding protein, iron compound transporter gi|170076609
ABC transporter permease gi|170077236
inorganic polyphosphate/ATP-NAD kinase [gi|170076848
ABC transporter ATP-binding protein gi|170079425
periplasmic binding protein, iron compound transporter gi|170076567
RecF/RecN/SMC domain-containing protein gi|170079221
lucB family siderophore biosynthesis protein gi|170076492
ABC transporter permease gi|170076549
cation-transporting P-type ATPase gi|170079204
ABC transporter ATP-binding protein gi|170076570
periplasmic binding protein; iron siderophore transporter system gi|170076572

FIGURE 3 | Heatmaps of protein abundance from triplicated biological treatments with low Fe (left columns) vs. when high Fe (right columns) was supplied to *Synechococcus* PCC 7002 during growth. Each protein was normalized to the average spectral abundance of that protein across all experiments. Red indicates more abundant, black is lower abundance. Proteins in bold are involved in Fe uptake or siderophore biosynthesis and/or import/export. Accession numbers are given for each protein.

rate, and two minimum peptides per protein (Keller et al., 2002). Numerous proteins involved in intracellular Fe homeostasis were detected in higher abundance when cells were grown with high Fe vs. low Fe, including ferrodoxin/thioredoxin proteins (**Figure 3**). Also present in high Fe treatments were higher levels of superoxide dismutase (SOD), and proteins involved in Photosystems I and II. In contrast, cells cultivated with 7.5 μM Fe(II) had higher levels of siderophores and Fe-transport proteins involved in Fe acquisition (**Table 4**), and recombinase proteins involved in DNA repair.

Fe(III) Mineral Precipitation during Fe(II) Oxidation by *Synechococcus* PCC 7002

SEM imaging revealed that Fe minerals produced by *Synechococcus* PCC 7002 were abundant relative to cells during the initial growth stage in a culture that still contained about 4000 μM Fe(II) from a total initial Fe(II) concentration of 4500 μM Fe(II), and that few cells were visible (**Figures 4A,B**). As cell numbers increased and Fe(II) decreased to 300 μM (similar to **Figure 2**), cells became visually more abundant relative to minerals in SEM (**Figure 4C**), and cell surfaces appeared bare. CLSM imaging gave further insight into the spatial distribution of Fe(III) around cells. In the hydrated state, cells were associated with mineral phases, but these did not appear to directly coat cell surfaces (**Figure 5**). Instead, all the cells were surrounded by Fe(III), which formed a capsular structure without evidence for mineralization from the reflection signal, consistent with the presence of a sorbed, soluble, or ligand-bound Fe(III) phase (**Figures 5E,F**, and Supplementary Video). X-ray diffraction (XRD) on Fe minerals formed in incubations were X-ray amorphous (data not shown), consistent with the production of a ferrihydrite-like phase.

Fe(II) Oxidation Rate during Growth of *Synechococcus* PCC 7002 under Ferruginous Conditions

The concentrations of Fe(II) and O_2 were measured through the course of the growth experiments at initial Fe(II) concentrations of 29, 577, and 4800 μM Fe(II) (**Figure 6A**). Oxygen was detectable during the course of the 29 and 577 μM experiments while Fe(II) was still present, but oxygen was below detection until all of the Fe(II) in the 4800 μM Fe(II) experiment had been oxidized. The detection limits for oxygen by our method are stated as 2.83 ± 0.14 μM by the manufacturer, so it is possible that a few μM oxygen was present during the course of the 4800 μM Fe(II) experiments, even while Fe(II) was still present. These data were used to calculate the maximum Fe(II) oxidation rate and O_2 production rate in each experiment (**Table 3**, **Figure 6B**), determined by linear regression of the last three Fe(II) concentration data points. We additionally estimated the Fe(II) oxidation rate using the equation (Singer and Stumm, 1970):

$$-d[\mathrm{Fe(II)}]/dt = k[\mathrm{Fe(II)}][\mathrm{O_2}][\mathrm{OH^-}]^2 \quad (1)$$

using the activities of Fe(II) and O_2, based on measured concentrations at each time point, such as are displayed in **Figure 6**. In Equation (1), k is the overall rate constant (8.0×10^{13} L^2 mol^{-2} atm^{-1} at 25°C). Estimated rates determined this way were on average one order of magnitude slower than those observed by loss of Fe(II) and calculated by regression (**Table 3**).

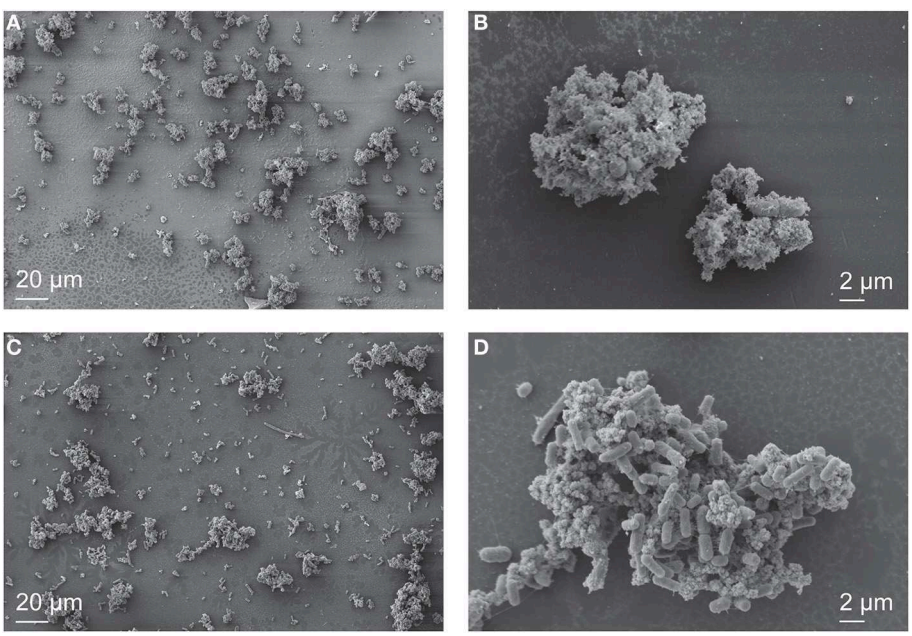

FIGURE 4 | SEM images of *Synechococcus* PCC 7002 cultured anoxically in 4500 μM Fe(II)-containing medium. In the early stages of growth, when 4000 μM Fe(II) remained in solution, individual cells are difficult to locate **(A)**, and the sample is predominantly composed of Fe minerals that surround the cells **(B)**. When nearly all the Fe(II) is oxidized (300 μM remains), cells are abundant **(C),** and cell surfaces are nearly free of Fe minerals **(D)**.

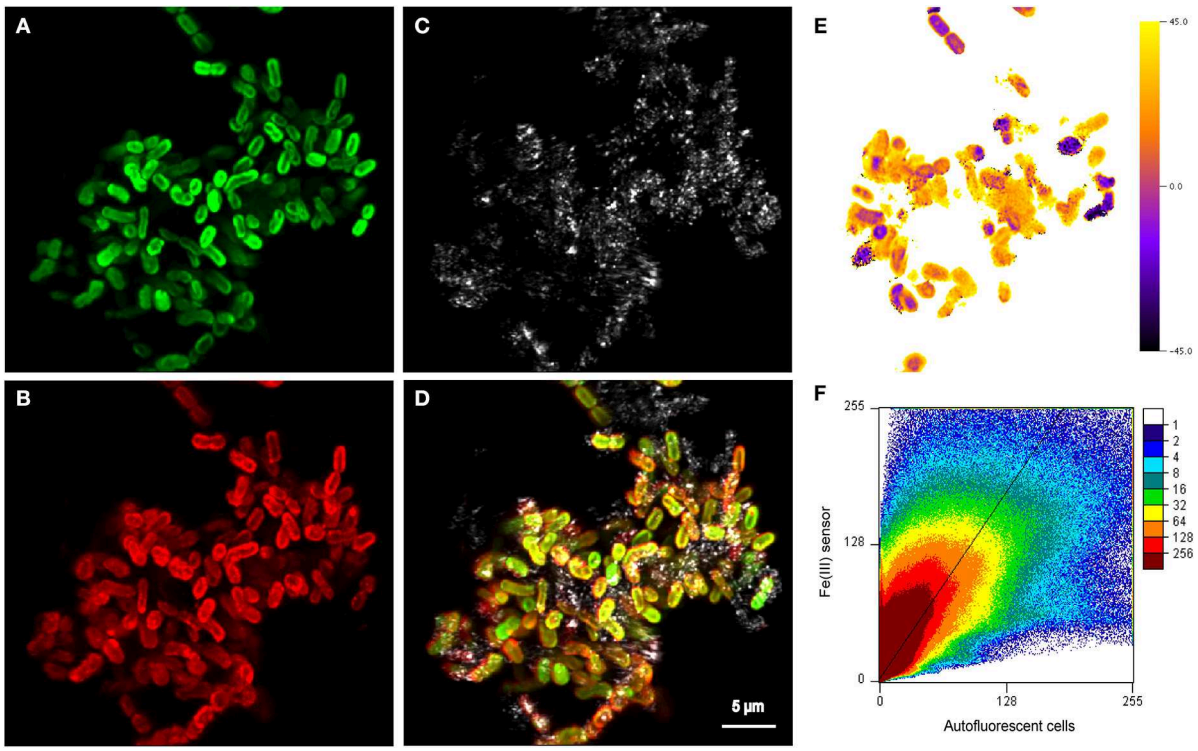

FIGURE 5 | Maximum projection of z-stacks collected on cell-mineral aggregates by CLSM showing (A) autofluorescent cells excited using the 635 nm laser, (B) distribution of sorbed Fe(III) stained with the Fe(III) sensor and excited with the 488 nm laser (Mao et al., 2007, 2010), (C) the reflection of the 488 nm laser showing the location of mineral phases, and (D) an overlay of all three channels. (E) Single slice of the 3D angle deviation map of the Fe(III) signal from **(B)** and the autofluorescence signal from **(A)**. An angle of 0° indicates that the fluorescence signals of the respective voxel would be located on the diagonal (slope = 1) in the scatterplot **(F)**. Positive angles indicate an enrichment of Fe(III), whereas negative angles could be caused by both a depletion of Fe(III) or a depletion of the Fe(III) fluorescence probe. To see all slices, see the Supplementary Video associated with this publication. The very broad distribution of values in the scatterplot **(F)** indicates a relatively poor spatial correlation of the Fe(III) signal with the autofluorescence signal, which is also confirmed by the relatively large root mean square error (RMSE) value of 11 of the reduced major axis regression with a slope >1 that is displayed. Units in **(F)** are normalized to the maximum signal of each channel.

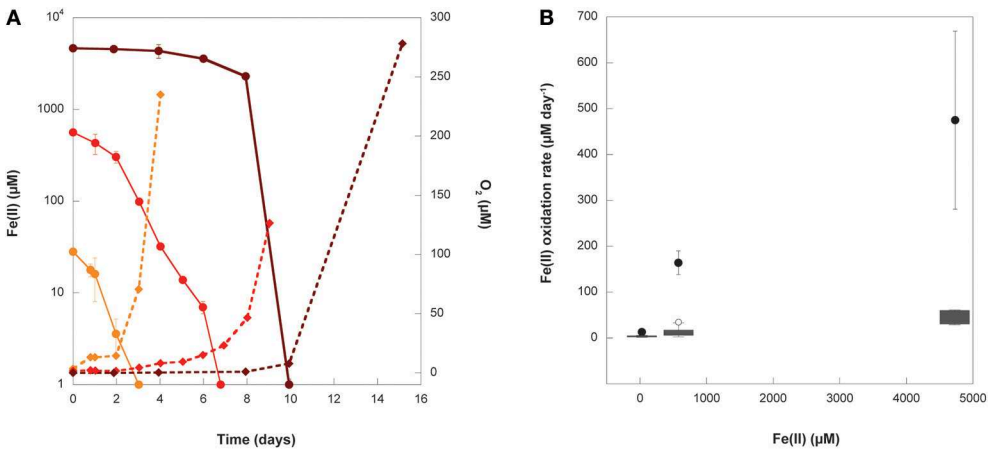

FIGURE 6 | (A) Fe(II) (circles) and O_2 (diamonds) measurements from representative replicates of experiments where *Synechococcus* PCC 7002 was grown under conditions that began anoxic with either 29 µM (orange), 577 µM (red), or 4732 µM (dark red) initial Fe(II). Error bars represent the standard deviation on replicated Fe(II) analyses from a single experiment. Error bars for O_2 are smaller than the symbols. **(B)** The Fe(II) oxidation rate calculated from linear regression (black circles) of data in **(A)** and the median, upper, and lower quartiles (gray boxes), range (whiskers), and outliers (open circles) of all oxidation rates calculated using Equation (1) for instantaneous measurements of Fe(II) and O_2 concentrations in **(A)** for each initial Fe(II) concentration.

TABLE 3 | Fe(II) oxidation and O_2 production rates for *Synechococcus* PCC 7002 in growth experiments that start anoxic with different initial concentrations of dissolved Fe(II).

Initial Fe(II) (μM)	n	Fe(II) oxidation rate (μM day^{-1})[b]	Fe(II) oxidation rate (μM day^{-1})[c]	O_2 production rate (μM day^{-1})[b]
7.5[a]	3	n.d.	n.d.	130 ± 91
29 ± 2	3	−13 ± 1	−0.019 to −0.092	120 ± 24
577 ± 14	3	−164 ± 26	−2.20 to −34.25	66 ± 34
4805 ± 458	3	−475 ± 194	−28 to −164	47 ± 9

Values indicate the average of biological replicates ± standard error (SE).
[a] Fe(II) added from trace element solutions.
[b] Rates were determined from linear regression of three data points with the steepest slopes.
[c] Rates were determined from Equation (1) and the maximum range for all biological experiments and instantaneous Fe(II) and O_2 measurements at a certain initial Fe(II) concentration. n.d., not determined.

Test for Anoxygenic Fe(II) Oxidation by *Synechococcus* PCC 7002

We tracked Fe(II) oxidation over 1 h in cell suspensions of *Synechococcus* PCC 7002 exposed to light with no DCMU (PSII in operation) vs. with DCMU (PSII blocked), in order to determine whether this strain could oxidize Fe(II) photosynthetically via a potential anoxygenic pathway of Photosystem I. DCMU is a herbicide that blocks electron transfer from Photosystem II to plastiquinone. Without DCMU, oxygen evolved from oxygenic photosynthesis increased through time, and Fe(II) concentrations decreased (**Figure 7A**). When DCMU was present, Fe(II) values were, within the analytical errors of the ferrozine assay, the same at the beginning and end of the experiment (**Figure 7B**).

Discussion

Physiological Response of *Synechococcus* PCC 7002 to Fe(II)

Growth Experiments

Because low Fe bioavailability is known to limit primary productivity in large expanses of the modern ocean (Boyd et al., 2000), and enhanced supply of Fe from atmospheric dust may have bolstered primary productivity in the past (the "Fe hypothesis") (Martin, 1990; Martínez-Garcia et al., 2014), it is generally thought that Fe additions to certain regions of the oceans can promote phytoplankton growth. At the opposite end of marine Fe concentrations are ferruginous conditions, where Fe(II) is stabilized in aqueous phase due to the higher solubility of Fe(II) than Fe(III) at circumnuetral pH under anoxic conditions. Interfaces where ferruginous waters meet an oxic photic zone were present in the Precambrian oceans (Holland, 1984), and also occur in modern oxygen minimum zones (OMZ) (Scholz et al., 2014). While the physiological effects of Fe limitation must be mitigated under ferruginous conditions, excess Fe could also have deleterious effects for organisms carrying out oxygenic photosynthesis, due to the production of ROS during chemical reactions between Fe(II) and oxygen. Previous work demonstrated that elevated Fe(II) concentrations (e.g., 100 s of μM) result in decreased growth rates in the marine cyanobacterium *Synechococcus* PCC 7002 (Swanner et al., 2015). Herein we document evidence that both low and high Fe concentrations can lead to decreased growth and cellular activity of *Synechococcus* PCC 7002, although likely for different physiological reasons under each condition, suggesting limits in terms of Fe concentrations and redox conditions that are relevant to the Fe hypothesis through geological time.

To explain the lowered growth rates for *Synechococcus* PCC 7002 with increasing initial Fe(II) concentrations (Swanner et al., 2015), it was suggested that toxicity arose from the production of ROS. Abiotic Fe(II) oxidation with O_2 generates ROS (O_2^-, H_2O_2, $OH^\cdot$) (Rush and Bielski, 1985). Extracellular ROS can oxidize membrane lipids of cyanobacteria (Morris et al., 2011). Intracellular ROS can oxidize DNA, RNA, proteins, and lipids (Cabiscol et al., 2000). Organisms utilize antioxidant enzymes such as superoxide dismutase (SOD) and catalase to remove ROS and its associated toxicity. In support of the role of ROS in Fe(II) toxicity, we observed that pigment levels decreased in response to elevated Fe(II) (**Table 1**). While carotenoids generally increase in response to elevated ROS, chlorophyll *a* and carotenoid levels may diminish due to degradation by ROS (Schäfer et al., 2005). Under Fe-limiting, oxic conditions using only Fe(III) as the Fe source, growth rates and pigment levels (including chlorophyll *a*) also decrease in this strain (Wilhelm et al., 1996). Together, these results show that *Synechococcus* PCC 7002 decreases its pigment levels in response to both Fe limitation and high Fe.

As evidence that Fe toxicity in *Synechococcus* PCC 7002 is specific to Fe(II) rather than Fe(III) or total Fe, we show that cell densities reached similar concentrations in incubations starting with 7.5 μM and 4800 μM Fe(II), once all of the Fe(II) oxidized and precipitated as Fe(III) minerals (**Figure 2**). These results suggest that toxicity effects cease once all Fe(II) is oxidized, likely due to the limited solubility of Fe(III) vs. Fe(II), and that toxicity only arises when Fe(II) is present at higher concentrations. Furthermore, previous experiments with *Synechococcus* PCC 7002 noted an increase in growth rates when total Fe(III) increased from 4.5 to 42 μM ($10^{-17.1}$ and $10^{-18.3}$ M dissolved Fe^{3+}, respectively) (Wilhelm et al., 1996), indicating that increasing Fe(III) concentrations stimulate growth rather than induce toxicity. These total Fe(III) concentrations are similar to those where toxic effects and diminished growth rates were noted with Fe(II) (tens to hundreds of micromolar; Swanner et al., 2015), consistent with Fe(II) as a toxic species.

Growth under anoxic conditions has also been documented for several laboratory strains of cyanobacteria, where decreased growth rates were linked to elevated CO_2 concentrations specifically rather than anoxic conditions generally (Thomas et al., 2005). In those experiments, *Synechococcus* PCC 7002 was able to grow in a 100% CO_2 atmosphere (Thomas et al., 2005). albeit more slowly than under ambient CO_2 concentrations (Hall et al., 1998). That finding suggests that *Synechococcus* PCC 7002 is adapted to higher CO_2 concentrations, as few common freshwater strains survive conditions of greater than 40% CO_2 (Thomas et al., 2005). The percentage of CO_2 in those experiments exceeded what was present in ours (10%), arguing against CO_2 toxicity in our experiments. The concentration of

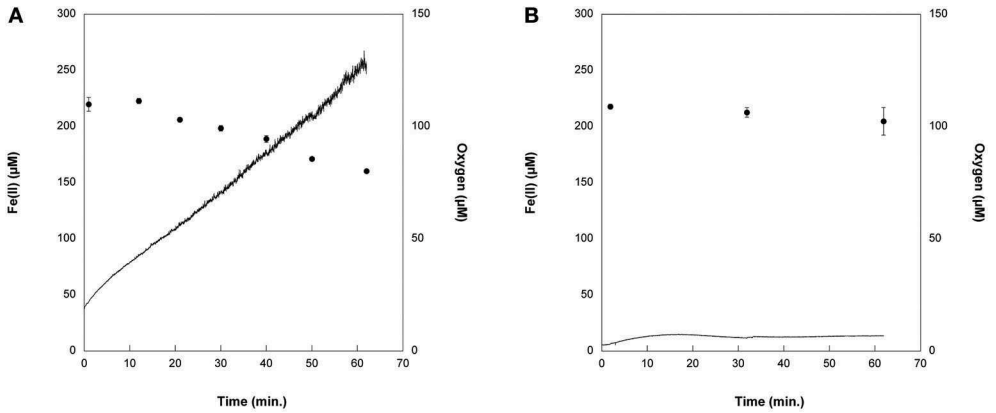

FIGURE 7 | Cell suspensions experiments with *Synechococcus* PCC 7002 (A) without DCMU, where Fe(II) (circles) was progressively oxidized as oxygen (solid line) was generated by photosynthesis, and (B) when DCMU was added. In the presence of DCMU, oxygen introduced to the cell stand during sampling can account for the minor amount of Fe(II) oxidation observed.

CO_2 in our experiments far exceeds modern atmospheric values, but CO_2 concentrations during the Archean were thought to be orders of magnitude higher than at present (Kasting, 1993; Sheldon, 2006). As our goal here is to understand the physiology of cyanobacteria in an Archean ocean, our experimental setup reasonably achieves this.

The O_2 production rate in our incubations decreased with increasing Fe(II) (**Table 3**). We reason that oxygen production is related to cellular growth, and that lowered oxygen production rates reflect lowered photosynthetic capacity as indicated by variable to maximum fluorescence ratios in *Synechococcus* PCC 7002 (Swanner et al., 2015). The exponential increase in O_2 only after all Fe(II) had been oxidized (**Figure 6A**) supports our interpretation that growth of *Synechococcus* PCC 7002 is inhibited only in the presence of Fe(II), and toxicity is mitigated once all Fe(II) is oxidized.

Proteomics Analysis

The low Fe [7.5 μM Fe(II)] treatment proteomic results reveal multiple responses to Fe scarcity, likely caused by the rapid oxidation of Fe(II) and precipitation of Fe(III) by photosynthetically derived oxygen coupled with the lack of resupply of Fe from a metal ion buffer (e.g., EDTA). Experimental observations of Fe(III) solubility at comparable media pH are ∼4 nM for total dissolved Fe (Kuma et al., 1996), and our culture experiments are likely similar or lower than this due to biological use. In the comparative analysis, more proteins were abundant in the low Fe relative to the high Fe [170 μM Fe(II)] treatment (Supplementary Table 1). This may reflect both deployment of multiple capabilities of this strain for confronting Fe limitation (i.e., production of siderophores) (Wilhelm and Trick, 1994), and a loss of any adaptive response to Fe(II) since cyanobacteria have not experienced ferruginous in recent geological history.

The production of Fe-binding siderophores was detected under Fe limitation in earlier studies with *Synechooccus* PCC 7002 (Wilhelm and Trick, 1994; Wilhelm et al., 1998). In particular, those studies observed a recovery of the growth rate once dissolved Fe^{3+} fell below $10^{-21.3}$ M, argued to be due to a corresponding increase in siderophore production (Wilhelm et al., 1996). Confirming the results of those prior studies, a number of siderophore biosynthesis proteins, TonB-dependent siderophore receptor proteins, and Fe transport-related proteins were more abundant in our low Fe treatment relative to the high Fe treatment (**Table 4**). TonB is also involved in the acquisition of other metal complexes (i.e., nickel, vitamin B_{12}) (Noinaj et al., 2010), and we cannot rule out that the expressed TonB proteins may be used for other metals. However, there were numerous Fe-specific transporters expressed, suggesting that our experimental conditions were indeed Fe limiting. ABC transporters, involved in import of Fe, siderophores, and heme groups in diverse bacteria and cyanobacteria (Köster, 2001; Hopkinson and Barbeau, 2012), were also abundant in the low Fe treatment, perhaps indicating the ability of this strain to take up diverse forms of Fe.

Iron transport proteins were also expressed in *Synechococcus* PCC 7002 in the high Fe treatment, but only one siderophore-related protein was detected under these conditions (**Table 4**). This suggests that siderophores are expressed under Fe limitation, and are not needed when abundant Fe is supplied as Fe(II). This nutritional role for Fe(II) is consistent with recent observations for uptake of Fe(II) in marine cyanobacteria (Kranzler et al., 2011; Lis et al., 2015). Furthermore, siderophores have much lower binding constants for Fe(II), and thus likely are not useful under these conditions (Neilands, 1995). ABC transporters, some of which were expressed in the high Fe treatment (**Table 4**), can also take up heme into the cell, which can bind either Fe(II) or Fe(III). This dataset cannot resolve whether or not these transporters were actually taking up excess Fe, as intracellular Fe quantification measurements utilized short-term incubations rather than growth experiments used for proteomics. The ferric uptake regulator (Fur) protein was more abundant in the high Fe treatment, and this protein is involved in repression of Fe uptake when intracellular Fe is sufficient (Bagg and Neilands, 1987). The low response of Fur to Fe(II) in this

TABLE 4 | Proteins putatively involved in Fe uptake or siderophore biosynthesis and/or uptake in *Synechococcus* PCC 7002, and their spectral abundance under low Fe [7.5 μm Fe(II)] or high Fe [170 μm Fe(II)].

Identified Proteins	Accession Number	7.5 μM Fe			170 μM Fe		
		a	b	c	a	b	c
Ferric uptake regulator	gi|170078257	0.0	2.4	2.5	5.3	8.6	7.6
Iron compound TonB-dependent receptor	gi|170077260	1.5	0.8	0.8	0.0	1.9	3.8
ABC transporter ATP-binding protein	gi|170077249	4.4	9.6	5.9	6.6	11.4	7.6
ABC transporter family protein	gi|170079375	4.4	3.2	0.8	1.3	1.9	1.9
ABC transporter ATP-binding protein	gi|170079425	2.9	2.4	2.5	0.0	1.0	3.8
ABC transporter ATPase	gi|170077798	5.8	8.8	4.2	0.0	6.7	3.8
ABC transporter family protein	gi|170078787	1.5	3.2	0.8	0.0	1.9	0.9
Na/H+ antiporter	gi|170077202	2.9	7.2	0.0	0.0	2.9	1.9
Iron transport protein	gi|170079102	68.7	53.5	57.8	26.3	25.7	19.8
IucB family siderophore biosynthesis protein	gi|170076492	0.0	3.2	2.5	1.3	1.0	0.0
ABC transporter ATP-binding protein	gi|170078821	7.3	3.2	1.7	0.0	1.0	1.9
TonB-dependent siderophore receptor	gi|170076608	100.9	96.7	142.3	7.9	4.8	10.4
Outer membrane TonB-dependent hemoglobin/transferrin/lactoferrin receptor family protein	gi|170076551	114.1	79.1	143.1	0.0	1.9	4.7
IucA/IucC family siderophore biosynthesis protein	gi|170076489	54.1	63.9	52.7	0.0	0.0	0.0
Ferrichrome-iron receptor; TonB-dependent siderophore receptor	gi|170076573	30.7	36.0	55.2	0.0	0.0	0.0
Siderophore biosynthesis protein	gi|170076493	30.7	36.8	25.1	0.0	0.0	0.0
TonB dependent receptor	gi|170076476	27.8	40.7	56.9	0.0	0.0	0.0
TonB-dependent siderophore receptor	gi|170076568	39.5	37.6	54.4	0.0	0.0	0.0
Cation-transporting P-type ATPase	gi|170079204	0.0	2.4	0.0	0.0	0.0	0.0
Siderophore biosynthesis protein; N-monooxygenase	gi|170076491	17.5	20.8	13.4	0.0	0.0	0.0
ABC transporter	gi|170077493	11.7	15.2	14.2	0.0	0.0	0.0
TonB family protein	gi|170076560	11.7	14.4	16.7	0.0	0.0	0.0
ABC transporter, periplasmic iron-binding lipoprotein	gi|170076553	20.5	24.0	26.8	0.0	0.0	0.0
Periplasmic binding protein, iron compound transporter	gi|170076609	17.5	5.6	5.9	0.0	0.0	0.0
Iron compound ABC transporter, ATP-binding protein	gi|170076550	4.4	5.6	4.2	0.0	0.0	0.0
ABC transporter permease	gi|170077236	2.9	0.8	0.8	0.0	0.0	0.0
ABC transporter ATP-binding protein	gi|170076570	0.0	1.6	0.0	0.0	0.0	0.0
Periplasmic binding protein, iron Compound transporter	gi|170076567	1.5	0.0	2.5	0.0	0.0	0.0
ABC transporter permease	gi|170076549	0.0	1.6	0.8	0.0	0.0	0.0
Periplasmic binding protein; iron siderophore transporter system	gi|170076572	0.0	1.6	0.0	0.0	0.0	0.0

study suggests that the Fe-sensing proteins such as the Fur system are not tied to expression of a metal detoxification system such as metallothionein in *Synechococcus* PCC 7002.

In support of the hypothesis that enhanced ROS are responsible for Fe(II) toxicity, the manganese enzyme superoxide dismutase (SOD), which dismutates superoxide (O_2^-) to either water or hydrogen peroxide (H_2O_2), was twice as abundant when cells were grown with high vs. low Fe (**Figure 3**). However, catalase-peroxidase HPI, which converts H_2O_2 to water, had similar abundance under both growth conditions. This could indicate that catalase is constitutively expressed, as it is in some bacteria (Hassett et al., 1992), while SOD expression is regulated by Fe concentrations. Expression of cyanobacterial Ni-containing SOD due to oxidative stress was previously linked to low Fe conditions (Saito et al., 2014). Also, light-driven Fenton chemistry consumes H_2O_2 as a reactant with Fe(II) (e.g., Zepp et al., 1992), such that superoxide may play a greater role than hydrogen peroxide in Fe toxicity. There were higher abundances of recombination proteins (i.e., *recA*) in the low vs. high Fe treatment, suggesting that general repair of damaged DNA mitigated by such proteins is more frequent under Fe limitation rather than due to Fe toxicity.

Further insights into the role of oxidative stress in the Fe toxicity observed for *Synechococcus* PCC 7002 come from some components of the photosynthetic pathways. PsaE, a subunit of photosystem I involved in stabilizing the electron carrier ferredoxin, was nearly twice as abundant in cells grown with high vs. low Fe. When PsaE was deleted in *Synechocystis* cells, there was upregulation of superoxide dismutase and catalase, higher intracellular ROS concentrations, and increased lipid peroxidation resulting from oxidative stress (Jeanjean et al., 2008). The conclusion of this study was that PsaE regulates leakage of electron from the electron transport chain back to oxygen, which generates ROS. Other studies have demonstrated that PsaE is involved in stabilizing the PSI/ferredoxin complex (Barth et al., 1998), which, when stabilized, may favor flow of electrons toward NADP vs. oxygen (Jeanjean et al., 2008), mitigating ROS production. A number of ferredoxin proteins were also more abundant in the high Fe treatment (**Figure 3**). Ferredoxins are key Fe-containing electron transfer proteins in

PSI, and increases in ferredoxin can help to mitigate excess electron transfer to oxygen, which generates ROS. Previous work with the cyanobacterial strain JSC-1, isolated from Fe-rich Chocolate Pots hot spring documented a high ratio of PSI:PSII (∼3.7; Brown et al., 2010). One possibility based on our results and the observation of Brown et al. (2010) is that cyanobacteria growing in the presence of Fe(II) may utilize PSI to transfer excess electrons to electron acceptors other than oxygen. PSII proteins could also be affected by oxidative stress. The PSII protein PsbU was more abundant in the high Fe treatment. Cyanobacterial mutants unable to make PsbU had lower variable fluorescence and oxygen yields, and it seems to play an important role in energy transfer in PSII (Veerman et al., 2005). As lower variable fluorescence and oxygen yields were characteristic of Fe(II) toxicity (Swanner et al., 2015), perhaps this protein is damaged by ROS, and must be synthesized in greater amounts to compensate, or expressing more of this protein helps to improve photosynthetic efficiency that is dampened by ROS (e.g., Swanner et al., 2015).

The electron-transfer mediating protein flavodoxin was more abundant in the low Fe experiment, although ferrodoxin was still present. Under Fe-limiting conditions, ferredoxin can be replaced by flavodoxin, which does not require Fe, in cyanobacteria and other phytoplankton (La Roche et al., 1996; Erdner et al., 1999). Ferredoxin and flavodoxin are important in mitigating oxidative stress, but increases in their abundance seems to occur on the order of days rather than hours (Mediavilla et al., 2010). These proteins are thus more likely to be important in mitigating oxidative stress in the growth experiments (**Figure 2** and Swanner et al., 2015), but not the short-term Fe-uptake experiments (**Table 2**) that were similar to experiments in which significant increases in intracellular ROS were detected (Swanner et al., 2015).

The high Fe treatment could have resulted in competitive inhibition with the uptake of other divalent cations, such as zinc, cobalt, and nickel, as observed for Fe(II) produced by reductases during cadmium uptake in phytoplankton (Lane et al., 2008). If this were occurring in our experiments, the production of intracellular metal detoxification proteins, such as metallothionein, might be expected, as observed in other marine cyanobacteria under high zinc and cadmium (Gupta et al., 1992; Cox and Saito, 2013). While metallothionein was not detected within the stringent conditions used to identify the 1631 proteins in this study, when the stringency was lowered to allow for only one peptide per protein identification, metallothionein was detected. This approach is reasonable for small proteins like metallothionein, which lacks multiple mass spectrometry amenable tryptic peptides within its protein sequence, where the 2-peptide rule penalizes smaller proteins. Interestingly, metallothionein did not show any notable increase in abundance under the high Fe treatment, instead showing a small reverse trend (1.66 vs. 0.33 spectral counts, respectively).

Fe Uptake and Sorption Experiments

Short-term (i.e., 1 h) incubations exposed cell suspensions of *Synechococcus* PCC 7002 to Fe(II) and light, and these incubations were used to track intracellular and sorbed Fe concentrations. Intracellular Fe contents were more than four times lower in the highest Fe treatments [i.e., 1000 μM Fe(II)] vs. the no Fe treatment (**Table 2**). These results are in contrast to previous experiments with *Synechococcus* PCC 7002, where more Fe was taken up into the cell as dissolved Fe concentrations increased either under oxic conditions with Fe(III) (Wilhelm et al., 1996), or when Fe(II) was supplied (Demirel et al., 2009). Notably, we lack a measurement of intracellular Fe contents prior to Fe exposure, but it is likely similar to the concentration of Fe in cells that were incubated with no additional Fe(II). One explanation for this phenomenon is that our Fe stock ($FeCl_2$) contains trace Cu, which could competitively bind to Fe uptake sites in this short-term incubation, preventing uptake of Fe(II). However, intracellular Cu levels were only slightly elevated in the highest Fe treatment (data not shown), giving little support to this line of reasoning. Alternatively, abundant Fe sorption and/or precipitation at the cell surface at higher Fe(II) concentrations (**Table 2**) could have blocked cellular transporters for Fe uptake. Fe sorbed to cyanobacteria surfaces was present in Fe(oxyhydr)oxide phases and bound to surface functional groups when Fe(II) was the Fe source at neutral pH (González et al., 2014), phases that might be less labile for uptake or block surface uptake sites.

The amount of Fe sorbed onto cell surfaces was double in the highest Fe treatments as compared to the cells where no Fe(II) was added (**Table 2**). In previous work, sorption of Fe to cyanobacterial extracellular polysaccharides (EPS) occurred within minutes (Demirel et al., 2009), consistent with the results of our short-term experiments. Sorbed Fe is a significant fraction (>10%) of total Fe in our short-term experiments (**Table 2**). Based on our detection of Fe(III) bound to the cell surface by CLSM (**Figure 5**), we suggest that as Fe(II) oxidized, Fe(III) is preferentially bound to surface functional groups rather than precipitated as Fe(III) oxyhydroxide minerals. This inference is supported by the localization of reflective minerals away from cell surfaces, and the detection of a soluble or ligand-bound Fe(III) phase at the cell surfaces (**Figure 5**). Previous experiments that looked at Fe sorption to cyanobacterial cell surfaces when Fe(II) was added found that only Fe(III) was bound (González et al., 2014). The phosphoryl groups of capsular EPS preferentially bind Fe(III) under neutral conditions, preventing growth of Fe(III) mineral polymers (González et al., 2014). Although EPS production has not been reported in *Synechococcus* PCC 7002 (De Philippis and Vincenzini, 1998), but this strain produces both hydroxamate and catechol-type siderophores (Wilhelm and Trick, 1994). Catechol-type siderophores are thought to be localized to the cell surface (Granger and Price, 1999), and although we did not see evidence for increased expression of siderophore proteins under ferruginous growth conditions, surface-associated catechol-type siderophores could have been produced under the conditions used to grow cells for the cell suspension experiments, where ferric ammonium citrate was the Fe source. Regardless of which type of organic moiety sorbs Fe at the cell surface, surface sorption may be a more significant fate for Fe(III) than Fe(III)-(oxyhdr)oxide mineral formation in this strain, as seems to be the case for diverse cyanobacteria (González et al., 2014).

Fe as a Sunscreen

Nanometer-scale Fe(III) (oxyhydr)oxide minerals, such as those produced during microbial Fe(II) oxidation, effectively absorb harmful UV radiation (Bishop et al., 2006). For this reason it is thought that prior to the development of an oxygenated atmosphere with an ozone layer, Fe minerals may have effectively protected early photosynthetic organisms from higher UV fluxes by serving as mineral "sunscreens" (Phoenix et al., 2001; Bishop et al., 2006). Additionally, aqueous Fe(III) shows enhanced UV absorption as compared to Fe(II) (Olson and Pierson, 1986). Fe(III) minerals could also serve as a sunscreen by physically covering cells. However, this advantage may be balanced by reduced growth if cell surfaces become coated with minerals that prevent the diffusion of nutrients (Kappler et al., 2005b; Klueglein et al., 2014), or if photosynthetically useful light is blocked by minerals. Despite the close association of minerals to *Synechococcus* PCC 7002 cells in SEM imaging (**Figure 4**), these samples were analyzed after critical point drying, and likely do not preserve the original spatial arrangement of Fe minerals to cells. Further imaging with CLSM reveals that cells of *Synechococcus* PCC 7002 that were grown with Fe(II) are not encrusted by minerals, but are coated by Fe(III) (**Figure 5**), which was visualized with a fluorescent sensor that only binds soluble or ligand-bound Fe(III) (Mao et al., 2007, 2010). This phase can be distinguished from Fe(III) associated with minerals, because fluorescence from the Fe(III)-ion-specific probe (**Figure 5B**) is not generally associated with the minerals visible in reflection (**Figure 5C**). The signal from the Fe(III)-ion specific probe is localized around the cell periphery (**Figure 5E** and Supplementary Video), in comparison to autofluorescent pigments (**Figure 5A**), which are generally found in the thylakoid, cell, and outer membranes (Vermaas et al., 2008). The angle-deviation increases from negative values in the cell center to positive values at the cell surface, indicating a depletion of either the Fe(III) fluorescence probe or Fe(III) in the cytoplasm and an accumulation of Fe(III) at the cell surface (**Figure 5E** and Supplementary Video). This finding is consistent with the interpretation that Fe(III) is sorbed (e.g., Section Fe Uptake and Sorption Experiments and **Table 2**), bound to cell-surface complexes.

Based on the lack of mineralization of the cell, it is unlikely that cell encrustation causes the decreased growth rates observed for this strain in the presence of Fe(II), a conclusion reached for non-photosynthetic Fe(II)-oxidizing bacteria (Klueglein et al., 2014). It is possible that the abundance of minerals in cultures (e.g., **Figure 1**) may also block light from reaching cell surfaces. Cyanobacteria cells can become chlorotic when light intensities are very low (Falkowski and Raven, 2007), possibly accentuating the rust-dominated color of the 4800 μM Fe(II) culture in **Figure 1**. An amorphous Fe mineral, likely ferrihydrite, was detected with XRD after Fe(II) oxidation by *Synechococcus* PCC 7002 (data not shown). Previous experiments with Fe(III) oxide minerals formed in the presence of oxygenic photosynthetic algae suggest that such phases are transparent to wavelengths of light needed for photosynthesis (Bishop et al., 2006), perhaps indicating that the presence of toxic Fe(II) is the ultimate cause of chlorosis (**Table 1**). As cell surface-associated Fe(III) was present in *Synechococcus* PCC 7002 cells (**Figure 5**), and was likely a ligand-bound Fe(III) (Mao et al., 2007, 2010; **Table 2**), it is possible that such a species could also serve as a sunscreen (Olson and Pierson, 1986). Finally, although the Fe-containing protein Dps may help to mitigate photooxidative stress due to ROS (Castruita et al., 2006), we did not see a large differential expression under low vs. high Fe treatments (**Figure 3**). Nor did we see expression of high-light inducible proteins known in *Synechococcus* PCC 7002 (Ludwig and Bryant, 2012) under the low or high Fe treatments.

Mechanism of Fe(II) Oxidation by *Synechococcus* PCC 7002

Some cyanobacteria are able to perform anoxygenic photosynthesis using sulfide as an electron donor as an alternative to oxygenic photosynthesis (Cohen et al., 1975; Garlick et al., 1977; Cohen, 1984). It has also been hypothesized that Fe(II), like sulfide, could serve as an electron donor for anoxygenic photosynthesis by cyanobacteria (Olson and Pierson, 1987b). This hypothesis stems from the similar redox potentials of the photosynthetic reactions center in cyanobacterial PSI to the reaction center used by purple bacteria, some of whom are able to utilize electrons transferred from Fe(II) (Widdel et al., 1993). Furthermore, molecular phylogenies indicate that purple and green bacteria and their anoxygenic photosystems evolutionarily predate cyanobacteria and oxygenic photosynthesis (Xiong, 2006), in which the photosystems of purple and green bacteria appear combined (Falkowski and Raven, 2007). Thus, it is possible that cyanobacteria retain the capability to use PSI for Fe(II)-dependent anoxygenic photosynthesis. Despite attempts to detect this process in isolates and within natural cyanobacterial populations (Pierson et al., 1999; Trouwborst et al., 2007), there is not clear evidence in the literature that any extant cyanobacterium is capable of such activity (see reference to unpublished report in Cohen et al., 1986). However, it will be important to determine if any cyanobacteria retain such a capability, which may indicate a temporal separation between the origin of cyanobacteria and the origin and utilization of oxygenic photosynthesis by cyanobacteria, and also a more direct role for cyanobacteria in deposition of oxidized Fe minerals to Precambrian BIF.

Some of the geochemical data collected during growth experiments with *Synechococcus* PCC 7002 can be used to infer whether anoxygenic photosynthesis using Fe(II) as the electron donor may have contributed to the Fe(II) oxidation observed. The simultaneous detection of O_2 and Fe(II) in our 29, 577, and 4800 μM Fe(II) experiments (**Table 3**, **Figure 6**) indicate a dependence of Fe(II) oxidation rate and O_2 production rate on initial Fe(II) concentrations. The maximum Fe(II) oxidation rate increased with increasing Fe(II) concentrations, consistent with a first-order dependence on Fe(II) concentrations observed in abiotic Fe(II) oxidation experiments (Singer and Stumm, 1970). The rates estimated using Equation (1) were lower than those calculated using linear regression (**Table 1**), which is likely because oxygen was being continually produced and reacting in our experiments, as compared to experiments from

which the rate equation was determined where oxygen was held constant (Singer and Stumm, 1970). Also, heterogeneous oxidation of Fe(II) at mineral surfaces could have enhanced the rate relative to what was calculated based on the Fe(II) and O_2 concentrations (Park and Dempsey, 2005). The Fe(II) oxidation rate by anoxygenic phototrophs is dependent on initial Fe(II) concentrations (Wu et al., 2014), and also light intensity, consistent with a maximum rate achieved when photosystems are fully saturated with light (Hegler et al., 2008; Wu et al., 2014). However, such dependence usually displays Michaelis-Menten kinetics (Hegler et al., 2008; Saraiva et al., 2012; Wu et al., 2014). More data points at higher Fe(II) concentrations would be needed to definitively say whether or not Michaelis-Menten kinetics are observed in **Figure 6**, however we have not been able to grow *Synechococccus* PCC 7002 at initial Fe(II) concentrations much higher than 4800 μM Fe(II), due to Fe(II) toxicity, and such experiments that would be needed to further evaluate whether Fe(II) oxidation follows Michaelis-Menten kinetics.

Further experiments were therefore needed to establish whether Fe(II) is utilized in anoxygenic photosynthesis by *Synechococcus* PCC 7002. In cell suspensions without DCMU, Fe(II) was oxidized progressively as oxygen was produced by photosynthesis (**Figure 7A**). When DCMU was added to cells, no oxygen was produced by *Synechococcus* PCC 7002 (data not shown). In experiments with DCMU and Fe(II) added to cells, 13 μM of Fe(II) was oxidized, a value within the errors of the Fe(II) determination (**Figure 7B**). However, 4.7 μM of oxygen entered the cell stand from the surrounding atmosphere during sampling. As each molecule of oxygen can oxidize four moles of Fe(II), this trace oxygen can account for any Fe(II) oxidation that did take place. These results support the interpretation that this strain cannot oxidize Fe(II) with a PSI-dependent pathway, but rather that oxygen is required to oxidize Fe(II).

A final criteria for evaluating whether *Synechococcus* PCC 7002 is capable of anoxygenic photosynthesis using Fe(II) as the electron donor is through available genomic and proteomic data. Photoferrotrophy, as well as other types of metabolic Fe(II) oxidation (and reduction) often make use of c-type cytochromes to transfer electrons to and from Fe(II). The proteins and cytochromes that have so far been implicated in Fe(II) oxidation share some homology and reversibility in electron-transfer activity with those identified from Fe(III)-reducing microbes (Liu et al., 2012; Shi et al., 2012). We did see enhanced expression of two c-type cytochromes in the proteomics experiments with high Fe(II) concentrations (accession numbers YP_001733383, 4EID_A; data not shown). We therefore performed a sequence search (Geneious 6.0.6) of the translated genome of *Synechococcus* PCC 7002 (accession number CP000951) using putative proteins implicated in electron transfer from Fe(II) in Fe(II)-oxidizing or Fe(III)-reducing microbes. The proteins *foxE* from *Rhodobacter ferrooxidans* sp. strain SW2 (accession number ABD36082), and *mtoA* from *Siderooxydans lithotrophicus* ES-1 (accession number YP_003525109) did not target any homologous proteins encoded by the *Synechococcus* PCC 7002 genome. The lack of homologous genes to known Fe(II) oxidases also casts doubt that other active or metabolic forms of Fe(II) oxidation, aside or in addition to photoferrotrophy (for instance, microaerophilic Fe(II) oxidation), are carried out by *Synechococcus* PCC 7002.

The Role of Cyanobacteria in an Fe-rich Early Earth

During the Precambrian, Fe(II) concentrations are estimated to have been as low as tens of μM, or as high as several mM in deep seawater (Eugster and Chou, 1973; Holland, 1973; Mel'nik, 1973; Morris and Horwitz, 1983; Canfield, 2005), and Fe(II) may have fluxed toward sunlit waters in upwelling currents (Holland, 1984; Beukes and Klein, 1992). As modern phytoplankton, including cyanobacteria, are most productive along coastal upwelling zones and where deep, nutrient-rich waters overturn, it is likely that Archean planktonic cyanobacteria would have experienced these Fe(II) fluxes in their habitat. It is thought that early oxygen was produced along coastal margins (Kendall et al., 2010; Planavsky et al., 2014), and that a chemical reaction between Fe(II) and oxygen is responsible for the oxidation of Fe(II) and deposition of Fe(III) minerals to BIF along the slope and occasionally shelf of these settings (Beukes and Klein, 1992; Beukes and Gutzmer, 2008). This is in part due to the interpretation that a chemocline where Fe(II) became oxidized was likely to have been below the photic zone, which would exclude light-dependent anoxygenic photosynthesis as a mechanism for Fe(II) oxidation, and rely rather on diffusion of an oxidant such as oxygen to depths below the photic zone (Smith, 2013). For these reasons, it seems warranted to take a fresh look at the original proposal by Cloud that cyanobacteria or other early oxygenic photosynthetic organisms were responsible for Precambrian Fe(II) oxidation and BIF deposition (1968), chemical sediments that form the cornerstone of data repositories on the nature of the early Earth's atmosphere and ocean. However, an important constraint on interpreting the role of different metabolic groups of bacteria on Precambrian Fe(II) oxidation is understanding if they produce distinct chemical, mineralogical, morphological or isotopic signatures in the presence of Fe(II), and how the presence of Fe in its different physical and chemical forms can regulate the productivity of different bacteria. Our investigations establish that *Synechococcus* PCC 7002 can further be used to evaluate some hypotheses regarding the formation and stabilization of oxidized Fe in the Precambrian oceans.

Proteomic data expand on the earlier observation that Fe(II) is toxic to cyanobacteria during oxygenic photosynthesis. The new data supports the hypothesis that toxicity arises from the production of intracellular ROS (e.g., Swanner et al., 2015), but highlights the role of certain PSI/PSII proteins in regulating ROS production, in addition to enhanced production of enzymes like SOD for ROS mitigation. Observations such as the toxicity of Fe(II) can be used to explore the efficiency with which cyanobacteria or other oxygenic phototrophs may have grown and/or produced oxygen in putative early Earth environments and ecosystems. Furthermore, an understanding of how these organisms respond to environmental stressors may inform further molecular phylogenetic reconstructions of their ancient counterparts, for instance which enzymes (e.g., superoxide dismutase, ferrodoxin, etc.) were necessary for the success of their

earliest relatives in Fe-rich environments that are a hallmark of the early Earth.

It is generally assumed that the earliest cyanobacteria were adapted to high dissolved Fe concentrations, due to their high demand for intracellular Fe relative to other organisms (Keren et al., 2004). By extension, ancient cyanobacteria may have possessed strategies to tolerate higher dissolved Fe, while modern cyanobacteria have adapted to life in environments with low dissolved Fe by developing sophisticated Fe acquisition systems (Wilhelm, 1995) or by replacing or removing Fe-dependent pathways (Rusch et al., 2010). Our proteome results generally validate this conclusion: a higher proteomic response was mounted to Fe limitation, suggesting that if early cyanobacteria did have large physiological response to deal with high Fe, those pathways may have been lost during the transition to an oxidized Earth surface. The proteome results do still support that Fe(II) toxicity to *Synechococcus* PCC 7002 seems to arise because of the presence of oxygen, and the potential for ROS to be generated from intermediates produced by PSII, although competitive inhibition of other divalent metals necessary for certain enzyme function is also a possibility. It is well-accepted that early cyanobacteria may have been poisoned by oxygen (Fridovich, 1998), especially via photosynthetic side reactions generating ROS (Falkowski and Raven, 2007), if they initially lacked a system for ROS scavenging (Cloud, 1968). MnSOD evolved early in the history of oxygenic photosynthesis (Wolfe-Simon et al., 2005), likely by the GOE at 2.4 Gy ago (Kirschvink et al., 2000). But in light of increasing evidence for oxygen production hundreds of millions of years prior to the GOE (Anbar et al., 2007; Wille et al., 2007; Kendall et al., 2010; Crowe et al., 2013; Reinhard et al., 2013; Planavsky et al., 2014), a further possibility is that the origin of oxygenic photosynthesis preceded the evolution of ROS scavenging mechanisms such as MnSOD by some time. Such a scenario would have left the earliest cyanobacteria more vulnerable to Fe(II) toxicity, especially in light of elevated Fe(II) concentrations in the oceans prior to the GOE, a possibility that may help to explain the lag in the rise of atmospheric oxygen after the first appearance of oxygen (Swanner et al., 2015). Elevated Fe(II), when present at interfaces or gradients with oxygen, could be a toxic scenario to life in general, as all the domains of life possess sophisticated ROS-defense systems, but still experience toxicity resulting from ROS (Imlay, 2013). The links between Fe, ROS and toxicity or pathogenesis likely extend to all of biology (Jomova et al., 2010; Flores et al., 2012; Vale-Costa et al., 2013).

Our investigations suggest that cells of *Synechococcus* PCC 7002 are not coated by Fe minerals, but that sorbed or ligand-bound Fe(III) at the cell surface could serve as a sunscreen. A consideration on the hypothesis that Fe minerals precipitated by cyanobacteria could act as a sunscreen is the removal of Fe minerals from the water column by sedimentation. Shallow platforms on continental shelves may have been an important habitat for early photosynthetic organisms (Sumner, 1997; Allwood et al., 2006), where minerals would have deposited to microbial mats or sediments within the photic zone. If Fe minerals were forming in intimate association with mat-forming cyanobacteria, such as has been observed at Chocolate Pots hot spring in Yellowstone National Park (Parenteau and Cady, 2010), they may serve as a better sunscreen. However, the most significant oceanoc regions for oxygen production may have been above deeper waters or open ocean (Olson et al., 2013; Swanner et al., 2015). In these settings, precipitated Fe minerals are more likely to be removed from the photic zone by sedimentation than in shallow waters where light still penetrates the sediments. Furthermore, removal of non-encrusted phototrophic cells associated with minerals increases as the amount of initial Fe(II):Fe minerals formed increases (Posth et al., 2010), a phenomenon that could balance any growth benefit in terms of UV protection. Therefore, benthic cyanobacteria were more likely to have benefitted more from any UV protective effects of Fe minerals as compared to planktonic cyanobacteria on the early Earth. The persistence of elevated total Fe concentrations in Archean and Proterozoic shallow-water carbonates relative to their Phanerozoic counterparts (Veizer et al., 1989; Wilson et al., 2010), suggest that Fe(II) reached the photic zone at carbonate platforms (Sumner and Grotzinger, 1996; Sumner, 1997). Archean-aged carbonates also host microfossils or sedimentary structures consistent with active microbial communities (Sumner, 1997; Allwood et al., 2006), although it is unclear if the oldest of these included organisms performing oxygenic photosynthesis (Bosak et al., 2009). These ambiguities suggest that if benthic communities included oxygenic photosynthetic bacteria, they could have experienced a range of effects from periodic Fe input to shallow water: from the beneficial "sunscreen" aspect to the detrimental toxicity effects of Fe(II)-induced ROS production.

After the discovery that modern photoferrotrophs are capable of anoxygenic photosynthesis with Fe(II) as the electron donor (Widdel et al., 1993), laboratory physiological studies demonstrated that these bacteria could have generated enough oxidized Fe to deposit the major Precambrian BIF without invoking the presence of cyanobacteria or other oxygenic phototrophs (Kappler et al., 2005a; Wu et al., 2014). The idea that photoferrotrophs were involved in Fe(II) oxidation and Fe(III) mineral deposition in the absence of atmospheric oxygen or in anoxic marine settings has pervaded the literature (Posth et al., 2013). However, our evolving understanding of the dynamics of atmospheric and marine oxygenation indicates that the role of cyanobacteria or other oxygenic phototrophs in these processes may need to be reconsidered. The spatial relationship of Fe minerals to cyanobacterial cells documented here may help to determine whether there are features that might distinguish cyanobacteria or other oxygenic phototrophs from other cell types retained in Fe-rich rocks. Other types of organisms expected to thrive in Fe-rich environments, such as microaerophilic Fe(II)-oxidizing bacteria, may show different patterns of mineralization, such as Fe-mineral coated filaments or twisted stalks that can be retained through geological time and low-grade metamorphic conditions (Krepski et al., 2013; Picard et al., 2015). A cyanobacterium isolated from Fe-rich Chocolate Pots hot spring in Yellowstone National Park accumulated intracellular Fe-phosphates (Brown et al., 2010), although any potential intracellular Fe minerals formed by *Synechococcus* PCC 7002 were too small to observe with the methods used here. Our observations indicate that one feature of this strain is the

accumulation of sorbed or ligand-bound Fe at the cell surface, which likely includes significant Fe(III) (**Table 3** and **Figure 5**). The extracellular Fe could be bound to capsular EPS at the cell surface (Zippel and Neu, 2011), or by catechol-type siderophores associated with the cell surface (Granger and Price, 1999), which are thought to be produced by this strain (Wilhelm and Trick, 1994; Wilhelm et al., 1996). Cell surface binding may distinguish Fe(III) oxidized by cyanobacteria from photoferrototrophs, who precipitate Fe(III) rather on organic material distal to cells (Miot et al., 2009; Wu et al., 2014), characteristics that may differentiate oxygenic from anoxygenic phototrophic cell remnants in the rock record. Our data also suggests that binding of Fe(III) at cyanobacterial cell surfaces may be at least as important as Fe(III) oxyhydroxide precipitation as a fate for Fe(III) (González et al., 2014).

The rates and mechanism of Fe(II) oxidation by *Synechococcus* PCC 7002 presented herein can be used to constrain both models of early Fe, O, and C cycling, as well as to provide context for what signatures of cyanobacteria or oxygenic phototrophs might remain in Fe-rich environments. For instance, our kinetic and cell suspension data point to a strictly abiotic, extracellular mechanism for Fe(II) oxidation for the strain *Synechococcus* PCC 7002. It is still necessary to investigate whether any other extant cyanobacteria may retain the ability to oxidize Fe(II) via an anoxygenic pathway. However, if no extant cyanobacteria are capable of anoxygenic photosynthesis using Fe(II), inferences regarding the earliest cyanobacteria may be made. One such inference might be that oxygenic photosynthesis is necessary for Fe(II) oxidation by cyanobacteria (i.e., that Fe(II) is only oxidized by a chemical reaction with oxygen). If this is the case, then the Fe:C ratios of Fe minerals deposited may have varied depending on the type of photosynthesis or metabolism employed. In terms of the Fe:C ratio, autotrophic, CO_2-fixing photoferrotrophs and microaerophilic FeOB are governed by a ratio of four moles of Fe oxidized per mole of C fixed. Although high Fe(II) conditions may limit growth of cyanobacteria and therefore the amount of C they can fix, there is no reason to expect such a stoichiometry between ferric Fe and organic C. Although further work is needed to quantify the effect of Fe(II) toxicity to C fixation and export, it is generally expected that more C could be fixed per mole of Fe oxidized from oxygenic vs. anoxygenic photosynthesis (cf. Köhler et al., 2013). Such distinctions may help to elucidate the biology responsible for the low concentrations (average <1 wt%) of organic carbon generally present in BIF (Klein and Beukes, 1992). Organic matter sedimented in the presence of Fe may be preserved on geological time scales (Lalonde et al., 2012), and organic matter preservation in BIF or other Fe-rich sediments could potentially arise from Fe-cell interactions (e.g., sorption) such as we describe. Experimental diagenesis and fieldwork in modern settings is useful to determine the fate of specific cell-mineral (or Fe) assemblages (Köhler et al., 2013; Cosmidis et al., 2014).

Conclusions

The higher abundances of Fe(II) in the oceans during Precambrian time necessitate an understanding of how cyanobacteria respond to elevated Fe(II) in terms of growth and oxygen production. Our growth experiments with *Synechococcus* PCC 7002 under initially anoxic, Fe(II)-rich conditions demonstrate that toxicity associated with oxygen production in the presence of Fe is a response to Fe(II), but not to Fe(III). The proteomic response of this organism to Fe limitation involves synthesis of many siderophores and other molecular Fe acquisition systems, consistent with the findings of previous studies. Under high Fe, when Fe is provided as Fe(II), there was not as extensive a proteomic response as to Fe limitation, suggesting that the proteomic response of cyanobacteria to elevated Fe(II) may have been lost as Fe(II)-rich conditions at the Earth's surface disappeared due to progressive oxidation. Nevertheless, the proteome produced under high Fe does support elevated ROS production as the toxic consequence of elevated Fe(II). We found no support from the genome or physiological experiments that this organism oxidizes Fe(II) via and enzymatic and/or photosynthetic pathway. Growth in the presence of Fe(II) resulted in extracellular Fe(III) mineralization, but also Fe(III) bound to organic moieties at the cell surface, which could include capsular EPS or catechol-type siderophores. This spatial distribution of Fe(III) around cells of cyanobacteria differs from what is observed in photoferrotrophs, and may be useful in distinguishing which organisms were responsible for precipitation of Fe to Precambrian BIF in any putative microbial fossils. Furthermore, our study indicates a complex role for Fe as a sunscreen for early cyanobacteria, dependent on both the form of Fe (e.g., mineral vs. complexed), the location relevant to the cell, and the habitat or environment (e.g., shelf/lagoon vs. upwelling/coastal).

Acknowledgments

Dr. Marion Eisenhut provided *Synechococcus* PCC 7002. Dr. Aude Picard and Nicholas Hagemann assisted with SEM sample preparation and imaging. Fabian Zeitvogel, Gregor Schmid, and Pablo Ingino for helpful advice in processing and interpreting CLSM data. Verena Hof, Markus Maisch, and Constantin Vogt and helped with cell counts. James Byrne made the XRD measurements. Prof. Britta Planer-Friedrich measured the intracellular Fe concentrations. Prof. Bettina Voelker gave helpful advice for evaluating the rates and kinetics of Fe(II) oxidation. EDS was supported by a National Science Foundation (NSF) International Research Fellowship (no. 1064391) and a Carl Zeiss Stiftung postdoctoral fellowship. MS was supported by the Gordon and Betty Moore Foundation and the NSF Chemical Oceanography program. AK was supported by the German Research Foundation (DFG, KA 1736/24-1), and by the European Research Council under the European Union's Seventh Framework Programme (FP/2007–2013)/ERC Grant, Agreement n. 307320–MICROFOX.

Supplementary Material

The Supplementary Material for this article can be found online at: http://journal.frontiersin.org/article/10.3389/feart.2015.00060

References

Abràmoff, M. D., Magalhães, P. J., and Ram, S. J. (2004). Image processing with IMAGEJ. *Biophotonics Int.* 11, 36–42. Available online at: http://www.imagescience.org/meijering/publications/download/bio2004.pdf

Allwood, A. C., Walter, M. R., Kamber, B. S., Marshall, C. P., and Burch, I. W. (2006). Stromatolite reef from the early Archaean era of Australia. *Nature* 441, 714–718. doi: 10.1038/nature04764

Anbar, A. D., Duan, Y., Lyons, T. W., Arnold, G. L., Kendall, B., Creaser, R. A., et al. (2007). A Whiff of oxygen before the great oxidation event? *Science* 317, 1903–1906. doi: 10.1126/science.1140325

Bagg, A., and Neilands, J. B. (1987). Ferric uptake regulation protein acts as a repressor, employing iron(II) as a cofactor to bind the operator of an iron transport operon in *Escherichia coli*. *Biochemistry* 26, 5471–5477. doi: 10.1021/bi00391a039

Barbeau, K., Rue, E. L., Bruland, K. W., and Butler, A. (2001). Photochemical cycling of iron in the surface ocean mediated by microbal iron(III)-binding ligands. *Nature* 413, 409–413. doi: 10.1038/35096545

Barbeau, K., Rue, E. L., Trick, C. G., Bruland, K. W., and Butler, A. (2003). Photochemical reactivity of siderophores produced by marine heterotrophic bacteria and cyanobacteria based on characteristic Fe(III) binding groups. *Limnol. Oceanogr.* 48, 1069–1078. doi: 10.4319/lo.2003.48.3.1069

Barbeau, K. (2006). Photochemistry of Organic Iron(III) complexing ligands in Oceanic Systems. *Photochem. Photobiol.* 82, 1505–1516. doi: 10.1111/j.1751-1097.2006.tb09806.x

Barth, P., Lagoutte, B. and Sétif, P. (1998). Ferredoxin reduction by Photosystem I from *Synechocystis* sp. PCC 6803: toward an understanding of the respective roles of subunits PsaD and PsaE in rerredoxin binding. *Biochemistry* 37, 16233–16241. doi: 10.1021/bi981379t

Bau, M., and Moeller, P. (1993). Rare earth element systematics of the chemically precipitated component in Early Precambrian iron formations and the evolution of the terrestrial atmosphere-hydrosphere-lithosphere system. *Geochim. Cosmochim. Acta* 57, 2239–2249. doi: 10.1016/0016-7037(93)90566-F

Bekker, A., Holland, H. D., Wang, P. L., Rumble, D. III, Stein, H. J., Hannah, J. L., et al. (2004). Dating the rise of atmospheric oxygen. *Nature* 427, 117–120. doi: 10.1038/nature02260

Beukes, N. J., and Gutzmer, J. (2008). Origin and paleoenvironmental significance of major iron formations at the Archean-Paleoproterozoic boundary. *SEG Rev.* 15, 5–47.

Beukes, N. J., and Klein, C. (1992). "Models for iron-formation deposition," in *The Proterozoic Biosphere: A Multidisciplinary Study*, eds J. W. Schopf and C. Klein (New York, NY: Cambridge University Press), 147–151.

Bishop, J. L., Louris, S. K., Rogoff, D. A., and Rothschild, L. J. (2006). Nanophase iron oxide as a key ultraviolet sunscreen for ancient photosynthetic microbes. *Int. J. Astrobiol.*5, 1–12. doi: 10.1017/S1473550406002886

Blank, C. E., and Sánchez-Baracaldo, P. (2010). Timing of morphologial and ecological innovations in the cyanobacteria - a key to understanding the rise in atmospheric oxygen. *Geobiology* 8, 1–23. doi: 10.1111/j.1472-4669.2009.00220.x

Blankenship, R. E. (1992). Origin and early evolution of photosynthesis. *Photosyn. Res.* 33, 91–111. doi: 10.1007/BF00039173

Bosak, T., Liang, B., Sim, M. S., and Petroff, A. P. (2009). Morphological record of oxygenic photosynthesis in conical stromatolites. *Proc. Natl. Acad. Sci. U.S.A.* 106, 10939–10943. doi: 10.1073/pnas.0900885106

Boyd, P. W., Watson, A. J., Law, C. S., Abraham, E. R., Trull, T., Murdoch, R., et al. (2000). A mesoscale phytoplankton bloom in the polar Southern Ocean stimulated by iron fertilization. *Nature* 407, 695–702. doi: 10.1038/35037500

Brown, I. I., Bryant, D. A., Casamatta, D., Thomas-Keprta, K. L., Sarkisova, S. A., Shen, G., et al. (2010). Polyphasic characterization of a thermotolerant *Siderophilic Filamentous* Cyanobacterium that produces intracellular iron deposits. *Appl. Environ. Microbiol.* 76, 6664–6672. doi: 10.1128/AEM.00662-10

Buick, R. (1992). The antiquity of oxygenic photosynthesis: evidence from stromatolites in sulphate-deficient Archaean lakes. *Science* 255, 74–77. doi: 10.1126/science.11536492

Cabiscol, E., Tamarit, J., and Ros, J. (2000). Oxidative stress in bacteria and protein damage by reactive oxygen species. *Int. Microbiol.* 3, 3–8.

Canfield, D. E. (1998). A new model for Proterozoic ocean chemistry. *Nature* 396, 450–453. doi: 10.1038/24839

Canfield, D. E. (2005). The early history of atmospheric oxygen: homage to Robert M. Garrels. *Annu. Rev. Earth Planet. Sci.* 33, 1–36. doi: 10.1146/annurev.earth.33.092203.122711

Castruita, M., Saito, M., Schottel, P. C., Elmegreen, L. A., Myneni, S., Stiefel, E. I., et al. (2006). Overexpression and characterization of an iron storage and DNA-binding Dps protein from *Trichodesmium erythraeum*. *Appl. Environ. Microbiol.* 72, 2918–2924. doi: 10.1128/AEM.72.4.2918-2924.2006

Cloud, P. E. Jr. (1968). Atmospheric and hydrospheric evolution on the primitive Earth: both secular accretion and biological and geochemical processes have affected earth's volatile envelope. *Science* 160, 729–736. doi: 10.1126/science.160.3829.729

Cohen, Y., Jorgensen, B. B., Padan, E., and Shilo, M. (1975). Sulphide-dependent anoxygenic photosynthesis in the cyanobacterium Oscillatoria limnetica. *Nature* 257, 489–492. doi: 10.1038/257489a0

Cohen, Y., Jørgensen, B. B., Revsbech, N. P., and Poplawski, R. (1986). Adaptation to Hydrogen Sulfide of Oxygenic and Anoxygenic photosynthesis among cyanobacteria. *Appl. Environ. Microbiol.* 51, 398–407.

Cohen, Y. (1984). "Oxygenic photosynthesis, anoxygenic photosynthesis, and sulfate reduction in cyanobacterial mats," in *Current Perspectives in Microbial Ecology,* eds M. J. Klug and C. A. Reddy. (Washington, DC: American Society for Microbiology), 435–441.

Conway, T. M., and John, S. G. (2014). Quantification of dissolved iron sources to the North Atlantic Ocean. *Nature* 511, 212–215. doi: 10.1038/nature13482

Cosmidis, J., Benzerara, K., Morin, G., Busigny, V., Lebeau, O., Jézéquel, D., et al. (2014). Biomineralization of iron-phosphates in the water column of Lake Pavin (Massif Central, France). *Geochim. Cosmochim. Acta* 126, 78–96. doi: 10.1016/j.gca.2013.10.037

Cox, A. D., and Saito, M. A. (2013). Proteomic responses of oceanic Synechococcus WH8102 to phosphate and zinc scarcity and cadmium additions. *Front. Microbiol.* 4:387. doi: 10.3389/fmicb.2013.00387

Crowe, S. A., Døssing, L. N., Beukes, N. J., Bau, M., Kruger, S. J., Frei, R., et al. (2013). Atmospheric oxygenation three billion years ago. *Nature* 501, 535–538. doi: 10.1038/nature12426

De Philippis, R., and Vincenzini, M. (1998). Exocellular polysaccharides from cyanobacteria and their possible applications. *FEMS Microbiol. Rev.* 22, 151–175. doi: 10.1111/j.1574-6976.1998.tb00365.x

Demirel, S., Ustun, B., Aslim, B., and Suludere, Z. (2009). Toxicity and uptake of iron ions by *Synechocystis* sp. E35 isolated from Kucukcekmece Lagoon, Istanbul. *J. Hazard. Mater.*171, 710–716. doi: 10.1016/j.jhazmat.2009.06.058

Dippon, U., Pantke, C., Porsch, K., Larese-Casanova, P., and Kappler, A. (2012). Potential function of added minerals as nucleation sites and effect of humic substances on mineral formation by the nitrate-reducing Fe(II)-oxidizer *Acidovorax* sp. BoFeN1. *Environ. Sci. Technol.* 46, 6556–6565. doi: 10.1021/es2046266

Erdner, D. L., Price, N. M., Doucette, G. J., Peleato, M. L., and Anderson, D. M. (1999). Characterization of ferredoxin and flavodoxin as markers of iron limitation in marine phytoplankton. *Mar. Ecol. Prog. Ser.* 184, 43–53. doi: 10.3354/meps184043

Eugster, H. P., and Chou, I.-M. (1973). The Depositional environments of precambrian banded iron-formations. *Econ. Geol.* 68, 1144–1168. doi: 10.2113/gsecongeo.68.7.1144

Falkowski, P. G., and Raven, J. A. (2007). *Aquatic Photosynthesis.* Princeton, NJ: Princeton University Press.

Flores, H. S., Wikfors, G. H., and Dam, H. G. (2012). Reactive oxygen species are linked to the toxicity of the *dinoflagellate Alexandrium* spp. to protists. *Aquat. Microbiol. Ecol.* 66, 199–209. doi: 10.3354/ame01570

Fridovich, I. (1998). Oxygen toxicity: a radical explanation. *J. Exp. Biol.* 201, 1203–1209.

Garlick, S., Oren, A., and Padan, E. (1977). Occurrence of facultative anoxygenic photosynthesis among filamentous and unicellular cyanobacteria. *J. Bacteriol.* 129, 623–629.

Gledhill, M., and Van Den Berg, C. M. G. (1994). Determination of complexation of iron(III) with natural organic complexing ligands in seawater using cathodic stripping voltammetry. *Mar. Chem.* 47, 41–54. doi: 10.1016/0304-4203(94)90012-4

González, A. G., Pokrovsky, O. S., Jiménez-Villacorta, F., Shirokova, L. S., Santana-Casiano, J. M., González-Dávila, M., et al. (2014). Iron adsorption onto soil

and aquatic bacteria: XAS structural study. *Chem. Geol.* 372, 32–45. doi: 10.1016/j.chemgeo.2014.02.013

Granger, J., and Price, N. M. (1999). The importance of siderophores in iron nutrition of heterotrophic marine bacteria. *Limnol. Oceanogr.* 44, 541–555. doi: 10.4319/lo.1999.44.3.0541

Gupta, A., Whitton, B. A., Morby, A. P., Huckle, J. W., and Robinson, N. J. (1992). Amplification and rearrangement of a prokaryotic metallothionein locus smt in *Synechococcus* PCC 6301 selected for tolerance to cadmium. *Proc. Biol. Sci.* 248, 273–281. doi: 10.1098/rspb.1992.0072

Hall, R. D., Currier, P. A., and Thomas, D. J. (1998). "Algal and cyanobacterial growth in 100% CO2," in *Gravitational and Space Biology Bulletin*, ed M. E. Musgrave (American Society for Gravitational and Space Biology), 19.

Haqq-Misra, J., Kasting, J. F., and Lee, S. (2011). Availability of O2 and H2O2 on Pre-Photosynthetic Earth. *Astrobiology* 11, 293–302. doi: 10.1089/ast.2010.0572

Hassett, D. J., Charniga, L., Bean, K. A., Ohman, D. E., and Cohen, M. S. (1992). Antioxidant defense mechanisms in *Pseudomonas aeruginosa*: resistance to the redox-active antibiotic pyocyanin and demonstration of a manganese-cofactored superoxide dismutase. *Infect. Immun.* 60, 328–336.

Hegler, F., Posth, N. R., Jiang, J., and Kappler, A. (2008). Physiology of phototrophic iron(II)-oxidizing bacteria: implications for modern and ancient environments. *FEMS Microbiol. Ecol.* 66, 250–260. doi: 10.1111/j.1574-6941.2008.00592.x

Holland, H. D. (1973). The Oceans: a possible source for iron in iron-formations. *Econ. Geol.* 68, 1169–1172. doi: 10.2113/gsecongeo.68.7.1169

Holland, H. D. (1984). *The Chemical Evolution of the Atmosphere and Oceans.* Princeton, NJ: Princeton University Press.

Hopkinson, B. M., and Barbeau, K. A. (2012). Iron transporters in marine prokaryotic genomes and metagenomes. *Environ. Microbiol.* 14, 114–128. doi: 10.1111/j.1462-2920.2011.02539.x

Horner, T. J., Williams, H. M., Hein, J. R., Saito, M. A., Burton, K. W., Halliday, A. N., et al. (2015). Persistence of deeply sourced iron in the Pacific Ocean. *Proc. Natl. Acad. Sci. U.S.A.* 112, 1292–1297. doi: 10.1073/pnas.1420188112

Imlay, J. A. (2013). The molecular mechanisms and physiological consequences of oxidative stress: lessons from a model bacterium. *Nat. Rev. Microbiol.* 11, 443–454. doi: 10.1038/nrmicro3032

Ionescu, D., Buchman, B., Heim, C., Hauesler, S., De Beer, D., and Polerecky, L. (2014). Oxygenic photosynthesis as a protection mechanism for cyanobacteria against iron-encrustation in environments with high Fe^{2+} concentrations. *Front. Microbiol.* 5:459. doi: 10.3389/fmicb.2014.00459

Jeanjean, R., Latifi, A., Matthijs, H. C. P., and Havaux, M. (2008). The PsaE subunit of photosystem I prevents light-induced formation of reduced oxygen species in the *cyanobacterium Synechocystis* sp. PCC 6803. *Biochim. Biophys. Acta* 1777, 308–316. doi: 10.1016/j.bbabio.2007.11.009

Jomova, K., Vondrakova, D., Lawson, M., and Valko, M. (2010). Metals, oxidative stress and neurodegenerative disorders. *Mol. Cell Biochem.* 345, 91–104. doi: 10.1007/s11010-010-0563-x

Kappler, A., Pasquero, C., Konhauser, K. O., and Newman, D. K. (2005a). Deposition of banded iron formations by anoxygenic phototrophic Fe(II)-oxidizing bacteria. *Geology* 33, 865–868. doi: 10.1130/G21658.1

Kappler, A., Schink, B., and Newman, D. K. (2005b). Fe(III) mineral formation and cell encrustation by the nitrate-dependent Fe(II)-oxidizer strain BoFeN1. *Geobiology* 3, 235–245. doi: 10.1111/j.1472-4669.2006.00056.x

Kasting, J. (1993). Earth's early atmosphere. *Science* 259, 920–926. doi: 10.1126/science.11536547

Keller, A., Nesviszhskii, A. I., Kolker, E., and Aebersold, R. (2002). Empirical statistical model to estimate the accuracy of peptide identifications made by MS/MS and database search. *Anal. Chem.* 74, 5383–5392. doi: 10.1021/ac025747h

Kendall, B., Reinhard, C. T., Lyons, T. W., Kaufman, A. J., Poulton, S. W., and Anbar, A. D. (2010). Pervasive oxygenation along late Archean ocean margins. *Nature Geosci.* 3, 647–652. doi: 10.1038/ngeo942

Keren, N., Aurora, R., and Pakrasi, H. B. (2004). Critical Roles of Bacterioferritins in iron storage and proliferation of cyanobacteria. *Plant Physiol.* 135, 1666–1673. doi: 10.1104/pp.104.042770

Kirschvink, J. L., Gaidos, E. J., Bertani, L. E., Beukes, N. J., Gutzmer, J., Maepa, L. N., et al. (2000). Paleoproterozoic snowball Earth: Extreme climatic and geochemical global change and its biological consequences. *Proc. Natl. Acad. Sci. U.S.A.* 97, 1400–1405. doi: 10.1073/pnas.97.4.1400

Klein, C., and Beukes, N. J. (1992). "Time distribution, stratigraphy, and sedimentologic setting, and geochemistry of precambrian iron-formation," in *The Proterozoic Bioshpere: A Multidisciplinary Biosphere,* eds J. W. Schopf and C. Klein (New York, NY: Cambridge University Press), 139–146.

Klueglein, N., Zeitvogel, F., Stierhof, Y.-D., Floetenmeyer, M., Konhauser, K. O., Kappler, A., et al. (2014). Potential role of nitrite for abiotic Fe(II) oxidation and cell encrustration during nitrate redution by denitrifying bacteria. *Appl. Environ. Microbiol.* 80, 1051–1061. doi: 10.1128/AEM.03277-13

Köhler, I., Konhauser, K. O., Papineau, D., Bekker, A., and Kappler, A. (2013). Biological carbon precursor to diagenetic siderite with spherical structures in iron formations. *Nat. Commun.* 4, 1741. doi: 10.1038/ncomms2770

Konhauser, K. O., Amskold, L., Lalonde, S. V., Posth, N. R., Kappler, A., and Anbar, A. D. (2007). Decoupling photochemical Fe(II) oxidation from shallow-water BIF deposition. *Earth Planet. Sci. Lett.* 258, 87–100. doi: 10.1016/j.epsl.2007.03.026

Köster, W. (2001). ABC transporter-mediated uptake of iron, siderophores, heme and vitamin B12. *Res. Microbiol.* 152, 291–301. doi: 10.1016/S0923-2508(01)01200-1

Kranzler, C., Lis, H., Shaked, Y., and Keren, N. (2011). The role of reduction in iron uptake processes in a unicellular, planktonic cyanobacterium. *Environ. Microbiol.* 13, 2990–2999. doi: 10.1111/j.1462-2920.2011.02572.x

Krepski, S. T., Emerson, D., Hredzak-Showalter, P. L., Luther Iii, G. W., and Chan, C. S. (2013). Morphology of biogenic iron oxides records microbial physiology and environmental conditions: toward interpreting iron microfossils. *Geobiology* 5, 457–471. doi: 10.1111/gbi.12043

Kuma, K., Nishioka, J., and Matsunaga, K. (1996). Controls on iron(III) hydroxide solubility in seawater: the influence of pH and natural organic chelators. *Limnol. Oceanogr.* 41, 396–407. doi: 10.4319/lo.1996.41.3.0396

La Roche, J., Boyd, P. W., Mckay, R. M. L., and Geider, R. J. (1996). Flavodoxin as an *in situ* marker for iron stress in phytoplankton. *Nature* 382, 802–805. doi: 10.1038/382802a0

Lalonde, K., Mucci, A., Ouellet, A., and Gélinas, Y. (2012). Preservation of organic matter in sediments promoted by iron. *Nature* 483, 198–200. doi: 10.1038/nature10855

Lane, E. S., Jang, K., Cullen, J. T., and Maldonado, M. T. (2008). The interaction between inorganic iron and cadmium uptake in the marine diatom *Thalassiosira oceanica*. *Limnol. Oceanogr.* 53, 1784–1789. doi: 10.4319/lo.2008.53.5.1784

Lis, H., Kranzler, C., Keren, N., and Shaked, Y. (2015). A comparative study of iron uptake rates and mechanisms amongst marine and fresh water cyanobacteria: prevalence of reductive iron uptake. *Life* 5, 841–860. doi: 10.3390/life5010841

Liu, J., Wang, Z., Belchik, S. M., Edwards, M. J., Liu, C., Kennedy, D. W., et al. (2012). Identification and characterization of MtoA: a decaheme *c*-type cytochrome of the neutrophilic Fe(II)-oxidizing bacterium *Sideroxydans lithotrophicus* ES-1. *Front. Microbiol.* 3:37. doi: 10.3389/fmicb.2012.00037

Lu, X., and Zhu, H. (2005). Tube-gel digestion: a novel proteomic approach for high throughput analysis of membrane proteins. *Mol. Cell Proteomics* 4, 1948–1958. doi: 10.1074/mcp.M500138-MCP200

Ludwig, M., and Bryant, D. A. (2012). *Synechococcus* sp. strain PCC 7002 transcriptome: acclimation to temperature, salinity, oxidative stress, and mixotrophic growth conditions. *Front. Microbiol.* 2:354. doi: 10.3389/fmicb.2012.00354

Mao, J., He, Q., and Liu, W. (2010). An rhodamine-based fluorescence probe for iron(III) ion determination in aqueous solution. *Talanta* 80, 2093–2098. doi: 10.1016/j.talanta.2009.11.013

Mao, J., Wang, L., Dou, W., Tang, X., Yan, Y., and Liu, W. (2007). Tuning the selectivity of two chemosensors to Fe(III) and Cr(III). *Org. Lett.* 9, 4567–4570. doi: 10.1021/ol7020687

Martin, J. H. (1990). Glacial-interglacial CO_2 change: the Iron Hypothesis. *Paleoceanography* 5, 1–13. doi: 10.1029/PA005i001p00001

Martínez-Garcia, A., Sigman, D. M., Ren, H., Anderson, R. F., Straub, M., Hodell, D. A., et al. (2014). Iron fertilization of the Subantarctic Ocean during the last ice age. *Science* 343, 1347–1350. doi: 10.1126/science.1246848

Mediavilla, M. G., Di Veneanzio, G. A., Guibert, E. E., and Tiribelli, C. (2010). Heterologous ferredoxin reductase and flavodoxin protect Cos-7 cells from oxidative stress. *PLoS ONE* 5:e13501. doi: 10.1371/journal.pone.0013501

Mel'nik, Y. P. (1973). Physical and *Chemical Conditions* of *Genesis* of Precambrian *Ferruginous Quartzites* Kiev: Inst. Geokhim. Fiz. Mineral. Akad Nauk Ukr. S.S.R

Miot, J., Benzerara, K., Obst, M., Kappler, A., Hegler, F., Schädler, S., et al. (2009). Extracellular iron biomineralization by photoautotrophic iron-oxidizing bacteria. *Appl. Environ. Microbiol.* 75, 5586–5591. doi: 10.1128/AEM.00490-09

Morris, J. J., Johnson, Z. I., Szul, M. J., Keller, M., and Zinser, E. R. (2011). Dependence of the cyanobacterium *Prochlorococcus* on hydrogen peroxide scavenging microbes for growth at the Ocean's Surface. *PLoS ONE* 6:e16805. doi: 10.1371/journal.pone.0016805

Morris, R. C., and Horwitz, R. C. (1983). The origin of the iron-formation-rich Hamersley Group of Western Australia—deposition on a platform. *Precambrian Res.* 21, 273–297. doi: 10.1016/0301-9268(83)90044-X

Neilands, J. B. (1995). Siderophores: structure and function of microbial iron transport compounds. *J. Biol. Chem.* 270, 26723–26726. doi: 10.1074/jbc.270.45.26723

Noinaj, N., Guillier, M., Barnard, T. J., and Buchanan, S. K. (2010). TonB-dependent transporters: regulation, structure, and function. *Annu. Rev. Microbiol.* 64, 43–60. doi: 10.1146/annurev.micro.112408.134247

Olson, J., and Pierson, B. (1987a). Origin and evolution of photosynthetic reaction centers. *Origins Life Evol. Biosph.* 17, 419–430. doi: 10.1007/BF02386479

Olson, J. M., and Pierson, B. K. (1986). Photosynthesis 3.5 thousand milliion years ago. *Photosyn. Res.* 9, 251–259. doi: 10.1007/BF00029748

Olson, J. M., and Pierson, B. K. (1987b). "Evolution of reaction centers in photosynthetic prokaryotes," in *International Review of Cytology,* eds K. W. J. G. H. Bourne and M. Friedlander (Academic Press), 209–248. doi: 10.1016/S0074-7696(08)61439-4

Olson, S. L., Kump, L. R., and Kasting, J. F. (2013). Quantifying the areal extent and dissolved oxygen concentrations of Archean oxygen oases. *Chem. Geol.* 362, 35–43. doi: 10.1016/j.chemgeo.2013.08.012

Parenteau, M. N., and Cady, S. L. (2010). Microbial biosignatures in iron-mineralized phototrophic mats at Chocolate Pots Hot Springs, Yellowstone National Park, United States. *Palaios* 25, 97–111. doi: 10.2110/palo.2008.p08-133r

Park, B., and Dempsey, B. A. (2005). Heterogeneous Oxidation of Fe(II) on Ferric Oxide at Neutral pH and a Low Partial Pressure of O2†. *Environ. Sci. Technol.* 39, 6494–6500. doi: 10.1021/es0501058

Partensky, F., Hess, W. R., and Vaulot, D. (1999). *Prochlorococcus*, a marine photosynthetic prokaryote of global significance. *Microbiol. Mol. Biol. Rev.* 63, 106–127.

Pavlov, A. A., and Kasting, J. F. (2002). Mass-Independent fractionation of Sulfur isotopes in Archean Sediments: strong evidence for an anoxic archean atmosphere. *Astrobiology* 2, 27–41. doi: 10.1089/153110702753621321

Pecoits, E., Smith, M. L., Catling, D. C., Philippot, P., Kappler, A., and Konhauser, K. O. (2015). Atmospheric hydrogen peroxide and Eoarchean iron formations. *Geobiology* 13, 1–14. doi: 10.1111/gbi.12116

Phoenix, V. R., Konhauser, K. O., Adams, D. G., and Bottrell, S. (2001). Role of biomineralization as an ultraviolet shield: implications for Archean life. *Geology* 29, 823–826. doi: 10.1130/0091-7613(2001)029<0823:ROBAAU>2.0.CO;2

Picard, A., Kappler, A., Schmid, G., Quaroni, L., and Obst, M. (2015). Experimental diagenesis of organo-mineral structures formed by microaerophilic Fe(II)-oxidizing bacteria. *Nat. Commun.* 6:6277. doi: 10.1038/ncomms7277

Pierson, B. K., Paranteau, M. N., and Griffin, B. M. (1999). Phototrophs in high-iron-concentration microbial mats: physiological ecology of phototrophs in an iron-depositing hot spring. *Appl. Environ. Microbiol.* 65, 5474–5483.

Planavsky, N. J., Asael, D., Hofmann, A., Reinhard, C. T., Lalonde, S. V., Knudsen, A., et al. (2014). Evidence for oxygenic photosynthesis half a billion years before the Great Oxidation Event. *Nat. Geosci.* 7, 283–286. doi: 10.1038/ngeo2122

Planavsky, N. J., Mcgoldrick, P., Scott, C. T., Li, C., Reinhard, C. T., Kelly, A. E., et al. (2011). Widespread iron-rich conditions in the mid-Proterozoic ocean. *Nature* 477, 448–451. doi: 10.1038/nature10327

Posth, N. R., Huelin, S., Konhauser, K. O., and Kappler, A. (2010). Size, density and composition of cell-mineral aggregates formed during anoxygenic phototrophic Fe(II) oxidation: Impact on modern and ancient environments. *Geochim. Cosmochim. Acta* 74, 3476–3493. doi: 10.1016/j.gca.2010.02.036

Posth, N. R., Konhauser, K. O., and Kappler, A. (2013). Microbiological processes in banded iron formation deposition. *Sedimentology* 60, 1733–1754. doi: 10.1111/sed.12051

Poulton, S. W., and Canfield, D. E. (2011). Ferruginous conditions: a dominant feature of the Ocean through Earth's History. *Elements* 7, 107–112. doi: 10.2113/gselements.7.2.107

Raven, J. A. (1990). Predictions of Mn and Fe use efficiencies of phototrophic growth as a function of light availability for growth and of C assimilation pathway. *New Phytol.* 116, 1–18. doi: 10.1111/j.1469-8137.1990.tb00505.x

Reinhard, C. T., Planavsky, N. J., and Lyons, T. W. (2013). Long-term sedimentary recycling of rare sulphur isotope anomalies. *Nature* 497, 100–103. doi: 10.1038/nature12021

Rusch, D. B., Martiny, A. C., Dupont, C. L., Halpern, A. L., and Venter, J. C. (2010). Characterization of Prochlorococcus clades from iron-depleted oceanic regions. *Proc. Natl. Acad. Sci. U.S.A.* 107, 16184–16189. doi: 10.1073/pnas.1009513107

Rush, J. D., and Bielski, B. H. J. (1985). Pulse radiolytic studies of the reactions HO2/O2- with Fe(II)/Fe(III) ions. The reactivity of HO2/O2- with ferric ions and its implications on the occurence of the Haber-Weiss Reaction. *J. Phys. Chem.* 89, 5062–5066. doi: 10.1021/j100269a035

Saito, M. A., Mcilvin, M. R., Moran, D. M., Goepfert, T. J., Ditullio, G. R., Post, A. F., et al. (2014). Multiple nutrient stresses at intersecting Pacific Ocean biomes detected by protein biomarkers. *Science* 345, 1173–1177. doi: 10.1126/science.1256450

Sakamoto, T., and Bryant, D. A. (1998). Growth at low temperature causes nitrogen limitation in the cyanobacterium *Synechococcus* sp. PCC 7002. *Arch. Microbiol.* 169, 10-19. doi: 10.1007/s002030050535

Sander, S. G., and Koschinsky, A. (2011). Metal flux from hydrothermal vents increased by organic complexation. *Nat. Geosci.* 4, 145–150. doi: 10.1038/ngeo1088

Saraiva, I. H., Newman, D. K., and Louro, R. O. (2012). Functional characterization of the FoxE iron oxidoreductase from the photoferrotroph *Rhodobacter ferrooxidans* SW2. *J. Biol. Chem.* 287, 25541–25548. doi: 10.1074/jbc.M112.360636

Schäfer, L., Vioque, A., and Sandmann, G. (2005). Functional *in situ* evaluation of photosynthesis-protecting carotenoids in mutants of the cyanobacterium Synechocystis PCC6803. *J. Photochem. Photobiol. B Biol.* 78, 195–201. doi: 10.1016/j.jphotobiol.2004.11.007

Schirrmeister, B. E., Gugger, M., and Donoghue, P. C. J. (2015). Cyanobacteria and the Great Oxidation Event: evidence from genes and fossils. *Palaeontology* 58, 769–785. doi: 10.1111/pala.12193

Schmid, G., Zeitvogel, F., Hao, L., Ingino, P., Floetenmeyer, M., Stierhof, Y.-D., et al. (2014). 3D analysis of bacterial cell-(iron)mineral aggregates formed during Fe(II) oxidation by the nitrate-reducting *Acidovorax* sp. strain BoFeN1 using complementary microscopy tomography approaches. *Geobiology* 12, 340–361. doi: 10.1111/gbi.12088

Scholz, F., McManus, J., Mix, A. C., Hensen, C., and Schneider, R. R. (2014). The impact of ocean deoxygenation on iron release from continental margin sediments. *Nat. Geosci.* 7, 433–437. doi: 10.1038/ngeo2162

Sheldon, N. D. (2006). Precambrian paleosols and atmospheric CO2 levels. *Precambrian Res.* 147, 148–155. doi: 10.1016/j.precamres.2006.02.004

Shi, L., Rosso, K. M., Zachara, J. M., and Fredericksson, J. K. (2012). Mtr extracellular electron-transfer pathways in Fe(III)-reducing or Fe(II)-oxidizing bacteria: a genomic perspective. *Biochem. Soc. Trans.* 40, 1261–1267. doi: 10.1042/BST20120098

Singer, P. C., and Stumm, W. (1970). Acidic mine drainage: the rate-determining step. *Science* 167, 1121–1123. doi: 10.1126/science.167.3921.1121

Smith, A. J. B. (2013). The composition and depositional environments of the mesoarchean iron formations of the West Rand Group of the Witwatersrand Supergroup, South Africa. *Econ. Geol.* 108, 111–134. doi: 10.2113/econgeo.108.1.111

Sorichetti, R. J., Creed, I. F., and Trick, C. G. (2014). Evidence for iron-regulated cyanobacterial predominance in oligotrophic lakes. *Freshw. Biol.* 59, 679–691. doi: 10.1111/fwb.12295

Stookey, L. L. (1970). Ferrozine - a new spectrophotometric reagent for iron. *Anal. Chem.* 42, 779–781. doi: 10.1021/ac60289a016

Sumner, D. Y., and Grotzinger, J. P. (1996). Were kinetics of Archean calcium carbonate precipitation related to oxygen concentrations? *Geology* 24, 119–122.

Sumner, D. Y. (1997). Carbonate precipitation and oxygen stratification in late Archean seawater as deduced from facies and stratigraphy of the Gamohaan and Frisco formations, Transvaal Supergroup, South Africa. *Am. J. Sci.* 297, 455–487. doi: 10.2475/ajs.297.5.455

Swanner, E. D., Mloszewska, A. M., Cirpka, O. A., Schoenberg, R., Konhauser, K. O., and Kappler, A. (2015). Modulation of oxygen production in Archaean oceans by episodes of Fe(II) toxicity. *Nat. Geosci.* 8, 126–130. doi: 10.1038/ngeo2327

Tang, D., and Morel, F. M. M. (2006). Distinguishing between cellular and Fe-oxide-associated trace elements in phytoplankton. *Mar. Chem.* 98, 18–30. doi: 10.1016/j.marchem.2005.06.003

Thomas, D. J., Sullivan, S. L., and Price, A. L. (2005). Common freshwater cyanobacteria grow in 100% CO_2. *Astrobiology* 5, 66–74. doi: 10.1089/ast.2005.5.66

Toner, B. M., Fakra, S. C., Manganini, S. J., Santelli, C. M., Marcus, M. A., Moffett, J. W., et al. (2009). Preservation of iron(II) by carbon-rich matrices in a hydrothermal plume. *Nat. Geosci.* 2, 197–201. doi: 10.1038/ngeo433

Trouwborst, R. E., Johnston, A., Koch, G., Luther Iii, G. W., and Pierson, B. K. (2007). Biogeochemistry of Fe(II) oxidation in a photosynthetic microbial mat: implications for Precambrian Fe(II) oxidation. *Geochim. Cosmochim. Acta* 71, 4627–4643. doi: 10.1016/j.gca.2007.07.018

Twining, B. S., and Baines, S. B. (2013). The Trace Metal Composition of Marine Phytoplankton. *Ann. Rev. Mar. Sci.* 5, 191–215. doi: 10.1146/annurev-marine-121211-172322

Twining, B. S., Baines, S. B., Fisher, N. S., and Landry, M. R. (2004). Cellular iron contents of plankton during the Southern Ocean Iron Experiment (SOFeX). *Deep Sea Res.* 51, 1827–1850. doi: 10.1016/j.dsr.2004.08.007

Vale-Costa, S., Gomes-Pereira, S., Teixeira, C. M., Rosa, G., Rodrigues, P. N., Tomás, A., et al. (2013). Iron overload favors the elimination of *Leishmani infantum* from mouse tissues through interaction with reactive oxygen and nitrogen species. *PLoS Neglected Trop. Dis.* 7:e2061. doi: 10.1371/journal.pntd.0002061

Van Baalen, C. (1962). Studies on marine blue-green algae. *Botanica Marina* 4, 129–139. doi: 10.1515/botm.1962.4.1-2.129

Van Den Berg, C. M. G. (1995). Evidence for organic complexation of iron in seawater. *Mar. Chem.* 50, 139–157. doi: 10.1016/0304-4203(95)00032-M

Veerman, J., Bentley, F. K., Eaton-Rye, J. J., Mullineaux, C. W., Vasil'ev, S., and Bruce, D. (2005). The PsbU Subunit of Photosystem II Stabilizes energy transfer and primary photochemistry in the Phycobilisome-Photosystem II Assembly of *Synechocystis* sp. PCC 6803†. *Biochemistry* 44, 16939–16948. doi: 10.1021/bi051137a

Veizer, J., Hoefs, J., Lowe, D. R., and Thurston, P. C. (1989). Geochemistry of Precambrian carbonates: II. Archean greenstone belts and Archean sea water. *Geochim. Cosmochim. Acta* 53, 859–871. doi: 10.1016/0016-7037(89)90031-8

Vermaas, W. F. J., Timlin, J. A., Jones, H. D. T., Sinclair, M. B., Nieman, L. T., Hamad, S. W., et al. (2008). *In vivo* hyperspectral confocal fluorescence imaging to determine pigment localization and distribution in cyanobacterial cells. *Proc. Natl. Acad. Sci. U.S.A.* 105, 4050–4055. doi: 10.1073/pnas.0708090105

Widdel, F., Schnell, S., Heising, S., Ehrenreich, A., Assmus, B., and Schink, B. (1993). Ferrous iron oxidation by anoxygenic phototrophic bacteria. *Nature* 362, 834–836. doi: 10.1038/362834a0

Widdel, F. (1980). *Anaerober Abbau von Fettsäuren und Benzosäure durch neu isolierte Arten.* Göttingen: Universitat Göttingen.

Wilhelm, S. W., Macauley, K., and Trick, C. G. (1998). Evidence for the importance of catechol-type siderophores in the iron-limited growth of a cyanobacterium. *Limnol. Oceanogr.* 43, 992–997. doi: 10.4319/lo.1998.43.5.0992

Wilhelm, S. W., Maxwell, D. P., and Trick, C. G. (1996). Growth, iron requirements, and siderophore production in iron-limited *Synechococcus* PCC 7002. *Limnol. Oceanogr.* 41, 89–97. doi: 10.4319/lo.1996.41.1.0089

Wilhelm, S. W., and Trick, C. G. (1994). Iron-limited growth of cyanobacteria: multiple siderophore production is a common response. *Limnol. Oceanogr.*39, 1979–1984. doi: 10.4319/lo.1994.39.8.1979

Wilhelm, S. W. (1995). Ecology of iron-limited cyanobacteria: a review of physiological responses and implications for aquatic systems. *Aquat. Microbial Ecol.* 9, 295–303. doi: 10.3354/ame009295

Wille, M., Kramers, J. D., Nägler, T. F., Beukes, N. J., Schröder, S., Meisel, T., et al. (2007). Evidence for a gradual rise of oxygen between 2.6 and 2.5 Ga from Mo isotopes and Re-PGE signatures in shales. *Geochim. Cosmochim. Acta* 71, 2417–2435. doi: 10.1016/j.gca.2007.02.019

Wilson, J. P., Fischer, W. W., Johnston, D. T., Knoll, A. H., Grotzinger, J. P., Walter, M. R., et al. (2010). Geobiology of the late Paleoproterozoic Duck Creek Fromation, Western Australia. *Precambrian Res.* 179, 135–149. doi: 10.1016/j.precamres.2010.02.019

Wolfe-Simon, F., Grzebyk, D., Schofield, O., and Falkowski, P. G. (2005). The role and evolution of superoxide dismutases in Algae1. *J. Phycol.* 41, 453–465. doi: 10.1111/j.1529-8817.2005.00086.x

Wu, J., and Luther Iii, G. W. (1995). Complexation of Fe(III) by natural organic ligands in the Northwest Atlantic Ocean by a competitive ligand equilibration method and a kinetic approach. *Mar. Chem.* 50, 159–177. doi: 10.1016/0304-4203(95)00033-N

Wu, W., Swanner, E. D., Hao, L., Zeitvogel, F., Obst, M., Pan, Y., et al. (2014). Characterization of the physiology and cell-mineral interactions of the marine anoxygenic phototrophic Fe(II)-oxidizer *Rhodovulum iodosum* - implications for Precambrian Fe(II) oxidation. *FEMS Microbiol. Ecol.* 88, 503–515. doi: 10.1111/1574-6941.12315

Xiong, J. (2006). Photosynthesis: what color was its origin? *Genome Biol.* 7:245. doi: 10.1186/gb-2006-7-12-245

Zeitvogel, F., Schmid, G., Hao, L., Ingino, P., and Obst, M. (2014). ScatterJ: an ImageJ plugin for the evaluation of analytical microscopy datasets. *J. Microsc.* doi: 10.1111/jmi.12187. [Epub ahead of print].

Zepp, R. G., Faust, B. C., and Hoigne, J. (1992). Hydroxyl radical formation in aqueous reactions (pH 3-8) of iron(II) with hydrogen peroxide: the photo-Fenton reaction. *Environ. Sci. Technol.* 26, 313–319. doi: 10.1021/es00026a011

Zippel, B., and Neu, T. R. (2011). Characterization of Glycoconjugates of extracellular polymeric substances in Tufa-Associated Biofilms by using fluorescence lectin-binding analysis. *Appl. Environ. Microbiol.* 77, 505–516. doi: 10.1128/AEM.01660-10

Conflict of Interest Statement: The authors declare that the research was conducted in the absence of any commercial or financial relationships that could be construed as a potential conflict of interest.